On the Effect of Thermal Cycles on the Tensile Behavior of Fiberglass Geogrid

Mohamed Shokr

A thesis submitted to McGill University
In partial fulfilment of the requirements of the degree of

Master of Engineering

Department of Civil Engineering
McGill University
Montreal, Quebec, Canada

December 2020

Abstract

Studying the effect of temperature cycles on the mechanical behavior of geosynthetic material is essential for the analysis and design of reinforced soil structures in cold climate. High-strength fiberglass geogrids are relatively new soil reinforcement materials that have improved properties with a potential for a wide range of applications. This research involves a preliminary experimental investigation that has been performed to examine the effect of temperature cycles on the response of two different biaxial geogrid materials, namely polymeric and stiff fiberglass geogrids. A total of seventy-two single ribs of the two types of geogrids were subjected to different thermal cycles and a series of tensile tests were performed to measure the ultimate strength and strain at failure for each sample. The experimental results are compared and the differences in mechanical properties of the two geogrid types are highlighted. Results indicated that, for the temperature from -28°C to 23°C, thermal cycles have minimal effects on the mechanical properties of both polymeric and stiff fiberglass geogrids. The results also showed that fiberglass geogrid presents superior mechanical properties with significantly lower strains at failure.

Résumé

L’étude de l’effet des cycles de température sur le comportement mécanique des matériaux géo synthétiques est essentielle pour l’analyse et la conception des ouvrages sur sols renforcés dans un climat froid.

Les géogrilles en fibre de verre à haute résistance sont des matériaux de renforcement de sol relativement nouveaux qui possèdent des propriétés améliorées ayant du potentiel pour une vaste panoplie d’applications.

Ce projet de recherche est une étude expérimentale préliminaire qui a été effectuée afin d’examiner de près les effets des cycles de température sur le comportement de deux géogrilles biaxiales différentes appelées: géogrilles en polymère et géogrille en fibre de verre rigide.

Les nervures simples de deux types de géogrilles ont été assujettis à différents cycles thermiques et une série d’essais de traction a été effectuée afin de mesurer la résistance ultime et le taux de défaillance pour chaque échantillon.

Les résultats expérimentaux sont comparés et les différences entre les propriétés mécaniques des deux types de géogrilles sont mises en évidence.

Les résultats ont indiqué, en tenant compte des différentes températures utilisées dans cette étude, que les cycles thermiques ont des effets minimes sur les propriétés mécaniques des géogrilles rigides en fibre de verre et en polymère. Il a par ailleurs été démontré que la géogrille rigide en fibre de verre possède des propriétés mécaniques supérieures, ayant des déformations moindres au moment de la défaillance.

Acknowledgements

First, I would like to deeply thank my supervisor, Prof. Mohamed A. Meguid for his support, guidance, patience, and encouragement.

Also, I’d like to acknowledge the support I received from all technical support stuff in the Civil Engineering Lab for their help throughout this experimental investigation.

I am deeply indebted to my family and friends for giving me all kind of supports I need.

Finally, a special thanks for Mitacs and Titan Environmental for the generous financial support.

Table of Contents

Abstract 1
Résumé 2
Acknowledgements 3
List of figures 6
List of tables 9
Chapter 1 Introduction 10
1.1 Background 10
1.2 Objective and Scope 11
1.3 Thesis Organization 11
Chapter 2 Literature review 13
2.1 Overview 13
2.2 Behavior of Geogrid and Geotextile at Low Temperature 13
2.3 Effects of Temperature on the Tensile Strength of Geogrids 16
2.4 Recent Geosynthetics applications in Cold Climates 18
2.5 Reinforced Embankment with Geotextile in Cold Temperature 22
2.6 Effect of Temperature on Fatigue of Polymers 24
2.7 Conclusions from the Literature Review 27
2.8 Motivation of this Research 28
Chapter 3 Experimental program 29
3.1 Introduction 29
3.2 Investigation the Effect of Thermal Cycles on Fiberglass Geogrid 30
3.2.1 Thermal Capacity 30
3.2.2 Tensile Tests 31
3.3 Investigating the Effect of Thermal Cycles on Polymeric Geogrid 42
3.3.1 Thermal Capacity 43
3.3.2 Tensile Tests 44
Chapter 4 Discussion and Comparison 55
4.1 Fiberglass Geogrid 55
4.1.1 Effect of Thermal Cycles on The Ultimate Strength 56
4.1.2 Effect of Thermal Cycles on Strains 57

4.1.3 Effect of Thermal Cycles on the Modulus of Elasticity 58
4.2 Polymeric Geogrid 59
4.2.1 Effect of Thermal Cycles on the Ultimate Strength... 60
4.2.2 Effect of Thermal Cycles on Strains 61
4.2.3 Effect of Thermal Cycles on the Modulus of Elasticity 61
4.3 Comparison between the tested Fiberglass and Polymeric Geogrids 62
4.3.1 Ultimate Strength for Single Rib 62
4.3.2 The Ultimate Strength per Meter 64
4.3.3 Ultimate Strain at Failure... 65
4.3.4 Modulus of Elasticity... 66
Chapter 5 Conclusion and Recommendation.. 67
5.1 Conclusions 67
5.2 Recommendations 68
References.. 69

List of figures

Figure 2.1 Reported uniaxial polyester result for Machine direction a) in 20°C b) in -20° C, (SGI19022.report.2020.03)........ 14

Figure 2.2 Tensile load- strain relations at temperature from 30°C to 50°C for HDPE geogrid (Kongkitkul et al., 2012)........ 15

Figure 2.3 Tensile load- strain relations at temperature from 30°C to 50°C for PET geogrid (Kongkitkul et al., 2012)........ 16

Figure 2.4 Temperature versus average tensile strength for the test geogrid 17

Figure 2.5 Tensile strength of tested woven geotextile samples under 20°C to 80°C (Koda et al., 2018) 18

Figure 2.6 (a) Shows poor ground condition (b) installing bi-axial geogrid over the weak subgrade (Bhat and Thomas, 2015) 19

Figure 2.7 Pavement configuration (Bhat et al.,2015)........ 20

Figure 2.8 (a) Placing granular subbase over the biaxial geogrid geotextile composite (b) Fiberglass grid installed over the first lift of asphalt concrete (Bhat et al.,2015)......... 20

Figure 2.9 Schematic of reinforced granular raft (Bhat et al.,2013)........ 21

Figure 2.10 Using high-strength geogrid as concrete reinforcement for sidewalk in Calgary, Canada (Bhat et al.,2019)........ 21

Figure 2.11 Conditions along the road right-of-way in April 2009........ 22

Figure 2.12 Embankment schematic diagram: (a) with geotextile (b) with geotextile and corduroy (Guzman and Alfaro, 2016)........ 24

Figure 2.13 Effect of temperature for PBT in the (a) longitudinal and (b) transverse directions and for PA6 in the (C) longitudinal and (d) transverse directions........ 26

Figure 2.14 Tensile strength of GFRP with different holding time and elevated temperature (Zhao and Wang 2018) ... 27
Figure 3.1. Temperature-time relationship for the fiberglass geogrid ... 30
Figure 3.2. (a) Supplied geogrid sheet; (b) Tested specimen ... 31
Figure 3.3. Details of the tensile test setup ... 33
Figure 3.4. Extensometer ... 34
Figure 3.5. Tension strain relation for zero cycle ... 36
Figure 3.6. Tension-strain relationship after four cycles ... 37
Figure 3.7. Tension-strain relationship after eight cycles ... 39
Figure 3.8. Tension-strain relationship after twelve cycles ... 40
Figure 3.9. Tension-strain relationship after sixteen cycles ... 41
Figure 3.10. Tension-strain relationship after twenty cycles ... 42
Figure 3.11. Polymeric geogrid Temperature-time curve ... 44
Figure 3.12.(a) Polymeric geogrid sheet (b) Tested specimen ... 45
Figure 3.13. Tension strain curve for zero cycle ... 47
Figure 3.14. Tension-strain relationship after four cycles ... 49
Figure 3.15. Tension-strain relationship after eight cycles ... 50
Figure 3.16. Tension-strain relationship for twelve cycles ... 51
Figure 3.17. Tension-strain relationship after sixteen cycles ... 52
Figure 3.18. Tension-strain relationship after twenty cycles ... 54
Figure 4.1 Ultimate strength for the tested single ribs in each tested cycle ... 57
Figure 4.2 Fiberglass geogrid ultimate strain for each tested cycle ... 58
Figure 4.3 Value of the fiberglass geogrid modulus of elasticity for each cycle ... 59

Figure 4.4 Ultimate strength for the tested single ribs 60

Figure 4.5 Polymeric geogrid ultimate strain for each tested cycle 61

Figure 4.6 Polymeric geogrid modulus of elasticity for each cycle 62

Figure 4.7 Fiberglass and polymeric geogrid strength-strain curve 63

Figure 4.8 Fiberglass and polymeric strength-strain relation 65

List of tables

Table 3.1. Conducted tests (Fiberglass geogrid) 29

Table 3.2. Results under room temperature (Zero thermal cycles) 35

Table 3.3. Sample response following four thermal cycles 37

Table 3.4. Sample response following eight thermal cycles 38

Table 3.5. Sample response following twelve thermal cycles 39

Table 3.6. Sample response after Sixteen thermal cycles 40

Table 3.7. Sample response following twenty thermal cycles 42

Table 3.8. Conducted tests (Polymeric geogrid) 43

Table 3.9. Results under room temperature (Zero thermal cycles) 46

Table 3.10. Sample response following four thermal cycles 48

Table 3.11. Sample response following eight thermal cycles 49

Table 3.12. Sample response following twelve thermal cycles 50

Table 3.13. Sample response following sixteen thermal cycles 52

Table 3.14. Sample response following twenty thermal cycles 53

Table 4.1. All the fiberglass geogrid recorded properties 55

Table 4.2. All the polymeric geogrid recorded properties 59

Table 4.3. Ultimate strength for fiberglass and polymeric geogrid for all thermal cycles 63

Table 4.4. Ultimate strength per meter for all tests 64

Table 4.5. Ultimate strain for all tests 65

Table 4.6. Modulus of elasticity for both the fiberglass and polymeric geogrids 66

Chapter 1

Introduction

1.1 Background

Soil reinforcement has become increasingly common in geotechnical engineering applications around the world with the availability of geosynthetic materials. This thesis compares the response of two different geogrid materials to tensile loading following exposure to short-term thermal cycles. These conditions represent what the geogrid would be subjected to as far as temperature variation in cold climate.

Numerous studies have been conducted to examine the effect of temperature change on the tensile strength and strains of geogrids. The literature review shows a number of experimental investigations that have been performed to measure the tensile strength of different types of geogrids under different temperature ranges. However, most of the conducted tests found in the literature cover a temperature range that does not allow for the compounding effect of the negative and positive temperatures to be examined. Moreover, previous studies are mostly limited to polymeric geogrids. Therefore, there is a need to expand these studies to cover the effect of thermal cycles on fiberglass geogrids.

To examine the mechanical behavior of fiberglass geogrid, a series of experiments have been conducted on 36 stiff fiberglass samples supplied by Titan Environment to measure the ultimate strength and strain at failure. Before testing, the samples were exposed to an increasing number of freeze-thaw cycles. Results are discussed and the measured properties are compared with 36 polymeric geogrid samples that were also exposed to identical freeze-thaw cycles. The results show that the tested fiberglass geogrid exhibits significantly lower strains compared to polymeric geogrid. Conclusions as well as recommendations are presented based on the experimental results.

To the author's knowledge, no studies have been performed to investigate the effect of freeze-thaw cycles on the tensile behavior of high-strength fiberglass geogrid.

1.2 Objective and Scope

The primary objective of the present study is to experimentally investigate the effect of thermal cycles on the ultimate strain and strength of both polymeric and fiberglass geogrid. The experimental results are then used to compare the behavior of each material under different thermal cycle.

Specific objectives of this research are:

- Review the available experimental investigations related to testing geogrid under different temperatures.
- Review the standard procedure relevant to tensile testing of single-rib geogrid materials.
- Carry out experiments to measure the thermal capacity of polymeric and fiberglass geogrids and compare the responses of the two materials.
- Carry out experiments to measure the tensile strength of geogrid samples after exposure to freeze-thaw cycles.
- Compare the results of the two tested geogrids and draw conclusions and recommendations based on the experimental results.

1.3 Thesis Organization

A brief description of each chapter included in the thesis is presented below.

In chapter (2) of this thesis, a review of the previous studies related to the use of geotextile at low temperature is presented.

Chapter (3) is divided into two sections. The first section presents the experimental program related to testing fiberglass geogrid, while the second section relates to the polymeric geogrid. Both sections cover the material properties, testing details, and procedure. Moreover, the test setup and the results obtained for both materials are also presented in this chapter.

Chapter (4) presents the discussion of the results as well as the comparison between the response of the two tested materials.

Chapter (5) presents the conclusion drawn from this study. It also includes the recommendations for further studies on the tensile behavior of fiberglass geogrid.

Chapter 2

Literature review

2.1 Overview

In geotechnical engineering, geosynthetics can be used as filters, drains, separators, hydraulic barriers and soil reinforcements (Palmeira, 2008). In cold regions, additional design considerations are needed to accommodate the environmental factors associated with low temperature, such as thaw settlement, and possible changes to the mechanical properties of the reinforcing material. Geosynthetics is one of the solutions used to stabilize earth structures during and after construction to mitigate potential problems related to low temperature.

2.2 Behavior of Geogrid and Geotextile at Low Temperature

Early studies focused on the effect of temperature on the behavior of geotextile. Calhoun (1972) reported the results of tensile tests performed on six polypropylenes geotextiles at temperatures ranging from -18°C to 82°C. It was concluded that the decrease in temperature resulted in a reduction in the sample elongation at failure. However, no significant effect on the tensile strength of the tested material was found in these experiments.

About ten years later, Allen (1983) conducted tensile tests on five different types of woven geotextiles (slit film polypropylene, needle punched polypropylene, heat bonded polypropylene, needle punched polyester and resin bonded polyester) subjected to different environmental conditions (e.g. dry, in fresh water, and in saline water) for temperatures that range from -12°C to 22°C. Little change in tensile strength was found under the investigated temperatures; however, the strain at failure decreased under low temperature except for the case of needle punched polyester geotextile.

SGI Testing Services reported in the report number SGI19022/2020, the tensile properties of 24 samples of uniaxial polyester (PET) geogrid (TE-UX200PET) in both the machine and cross-machine directions under temperatures of 20°C ±2°C (room temperature) and -20°C. For the below zero temperature testing, specimens were placed in a freezer at -20°C for 48 hours then tested immediately after removal from the freezer. Testing took three minutes from the removal time from the freezer to the completion of the required tests. (Figure 2.1a) shows the room temperature test result with an average ultimate tension and strain of 260 kN/m and 12.6%, respectively. While under -20 °C temperature (Figure 2.1b), both ultimate tension and ultimate strain reduced to 240 kN/m and 12%, respectively. Results showed a decrease in tensile strength and strains at failure with the decrease in temperature in both directions.

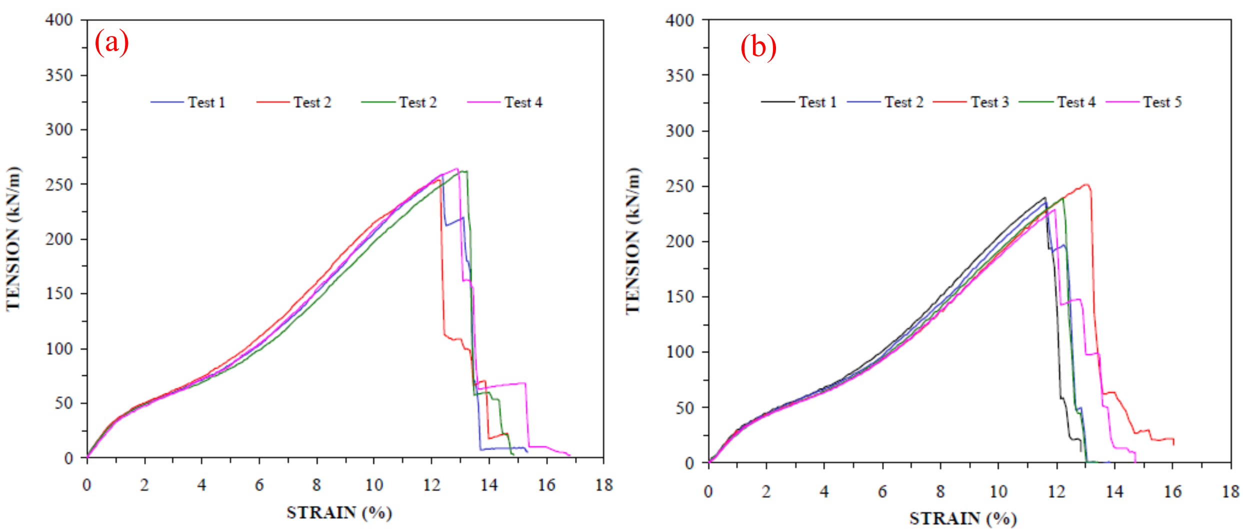

Figure 2.1 Reported uniaxial polyester result for Machine direction a) in 20°C b) in -20° C, (SGI19022/2020)

Kongkitkul et al. (2012) performed a series of tensile loading tests on three different types of polymeric geogrid: polypropylene (PP), high-density polyethylene (HDPE) and polyester (PET) following ASTM D 4595 test method. Tests were done inside a temperature-controlled chamber 64 cm high by 50 cm wide by 35 cm deep. The specimen's initial length was approximately 24 cm and the temperature ranged from 30°C to 50°C. The rate of temperature increase inside the chamber was 2°C per minute until reaching the target temperature, then was held constant for 2 hours to allow the specimen to settle. Figure 2.1 and 2.2 show the tension- strain relation for HDPE, and PET geogrid, respectively. The results as shown in the two figures indicate that, when the temperature increases from 30°C to 50°C, the tensile strength and elastic stiffness decreased by 26.7% and 4.5% for HDPE, and PET geogrid, respectively.

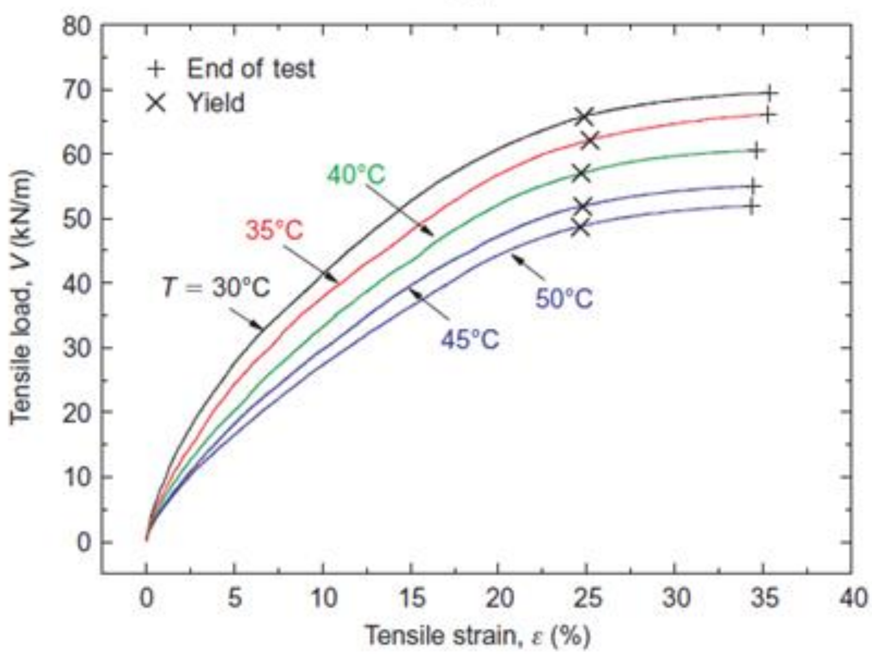

Figure 2.2 Tensile load- strain relations at temperature from 30°C to 50°C for HDPE geogrid (Kongkitkul et al., 2012)

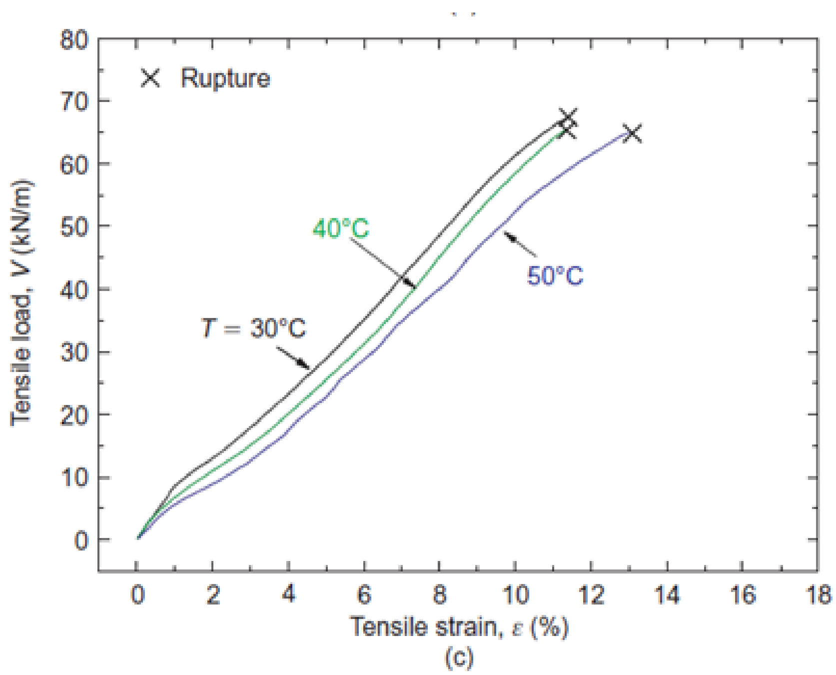

Figure 2.3 Tensile load- strain relations at temperature from 30°C to 50°C for PET geogrid (Kongkitkul et al., 2012)

2.3 Effects of Temperature on the Tensile Strength of Geogrids

Tests on PVC coated polyester geogrid were carried by Hsieh and Tseng (2008) under temperatures ranging from 0 °C to 80 °C following ASTM D6637-B. The sample used was 100 mm in width and consisted of three longitudinal ribs. A total of six samples were tested and the results revealed that the sample strength decreases with the increase in temperature. Figure 2.4 shows the temperature versus average tensile strength for all tested samples. The strength was found to decrease from 130 kN/m at 0°C to about 90 kN/m at 80°C. The rate of change in strength is found to be about -0.33% per degree Celsius.

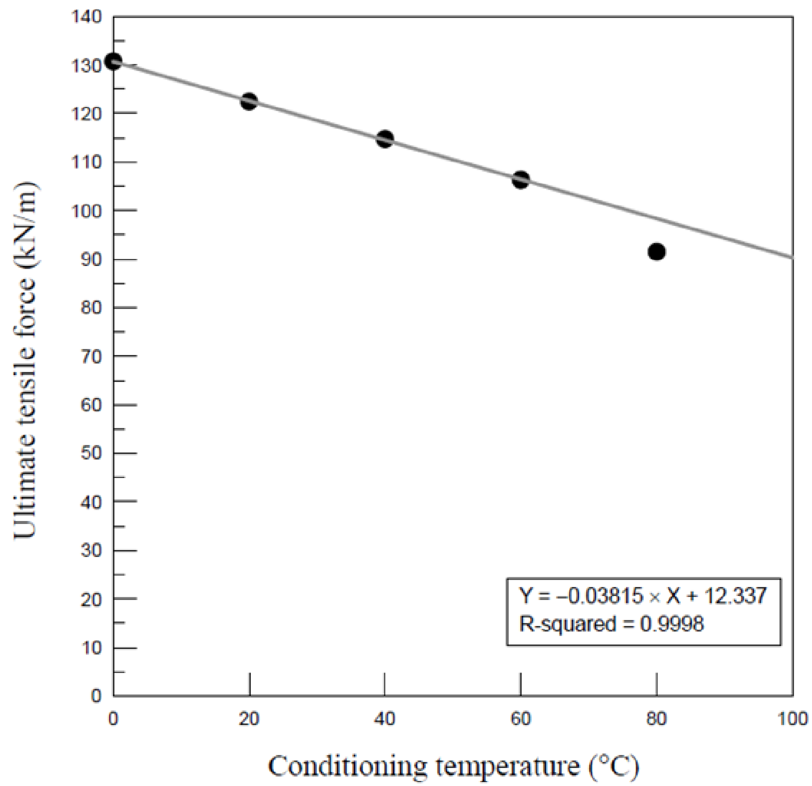

Figure 2.4 Temperature versus average tensile strength for the test geogrid (Hsieh and Tseng, 2008)

Koda et al. (2018) tests, following ISO 10319, five other samples for temperatures: 20°C, 50°C and 80°C reaffirmed the inverse proportionality between tensile strength and temperature. Figure 2.5 represents respectively in the horizontal and vertical axis the testing temperature and tensile stress. The highest tensile strength value was found to be 21.54 kN/m at 20°C while at 80°C the tensile strength decreased to 14.3 kN/m. Therefore, the tensile strength had decreased by 34% when the temperature rose from 20°C to 80°C.

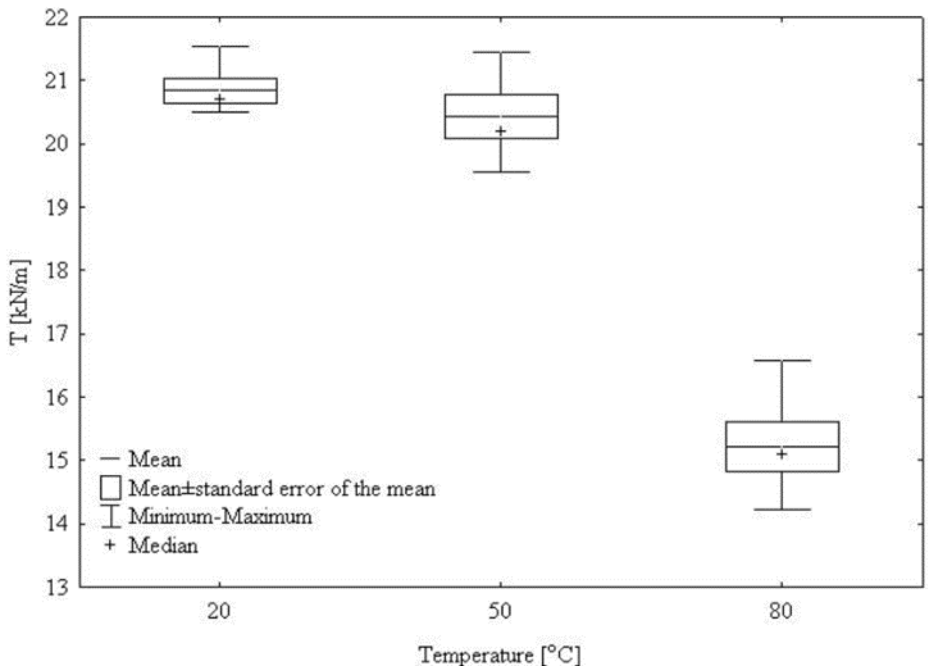

Figure 2.5 Tensile strength of tested woven geotextile samples under 20°C to 80°C (Koda et al., 2018)

2.4 Recent Geosynthetics applications in Cold Climates

Biaxial geogrid was used to reinforce an additional 6-track extension at Winnipeg. On these tracks, the heavy rail cars were expected to pass over soft and wet clay swampy subgrade (Figure 2.6a). One optimum solution was to place a single layer of robust bi-axial polymer geogrid composite over the weak saturated subgrade (Figure 2.6b). This solution was environmentally friendly as well as effective in reducing settlement (Bhat and Thomas, 2015).

Figure 2.6 (a) Shows poor ground condition (b) installing bi-axial geogrid over the weak subgrade (Bhat and Thomas, 2015)

On another project in Calgary, it was required to replace old damaged roads which were in distressed state as part of a roads-rehabilitation program. The proposed solution required replacement of the existing deteriorated pavement with a design including asphaltic concrete, granular base and sub-base. The process required to minimize the excavation depth to reduce the disruptions and inconvenience to the road users. For that, it was necessary to minimize the pavement thickness. The solution introduced using geosynthetics as pavement reinforcement to enhance the stiffness and strength of the pavement. Therefore, the reinforced pavement with lower thickness can give the same performance level as an unreinforced pavement. To satisfy all the requirements with respect to structural number and the minimum layer thickness, the pavement configuration was finalized as shown in figure 2.7 with biaxial geogrid and fiberglass grid (ultimate tensile strength of 31 kN/m and 100 kN/m, respectively).

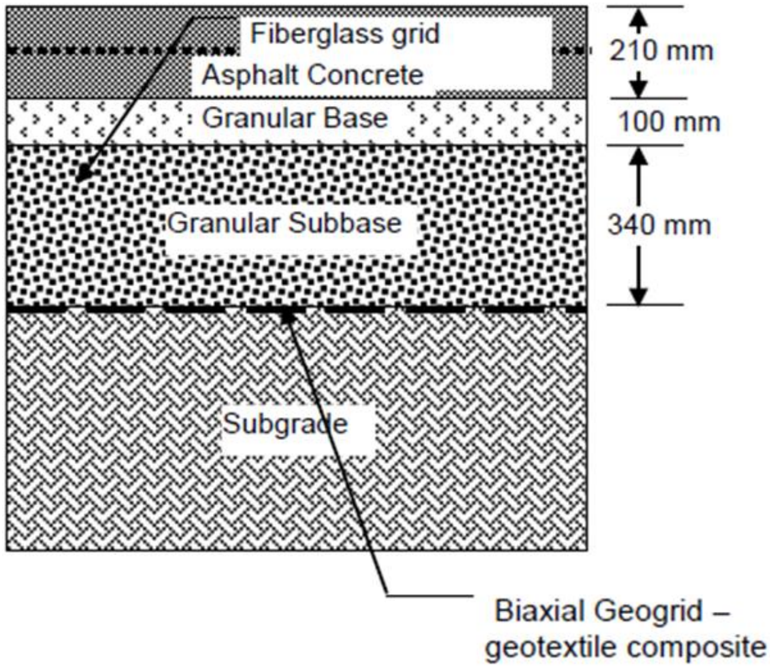

Figure 2.7 Pavement configuration (Bhat et al.,2015)

The biaxial geogrid was installed on the top surface of the excavated subgrade Figure 2.8a, while the fiberglass grid was laid over the second lift of asphalt concrete Figure 2.8b. with geosynthetic reinforcement incorporation, significant reduction in pavement thickness and depth excavation were obtained which minimized the problems during construction (Bhat et al.,2015).

Figure 2.8 (a) Placing granular subbase over the biaxial geogrid geotextile composite (b) Fiberglass grid installed over the first lift of asphalt concrete (Bhat et al.,2015).

On an additional project in northern Manitoba, Canada, the differential settlement was successfully controlled by reinforcing the granular pad of prefabricated water storage tanks with polymeric geogrid. The construction was completed by the end of 2012 with no indications of shear failure or excessive settlements so far. Figure 2.9 shows the schematic of reinforced granular raft with geotextile (Bhat et al.,2013).

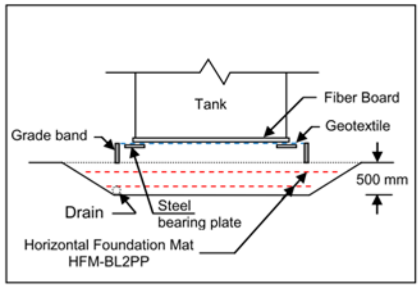

Figure 2.9 Schematic of reinforced granular raft (Bhat et al.,2013)

The geosynthetic applications are extended to reinforced concrete. As a pilot project in City of Calgary, high-strength geogrid was used as alternate to conventional steel for sidewalk reinforcement. The case study showed the use of fiberglass geogrid in 125 mm thick concrete sidewalk slab as shown in Figure 2.10. The main purpose was to increase the life cycle of the sidewalk by controlling the shrinkage cracking on the surface. After three winter cycles, the visual inspection showed no surface cracking in any sidewalk section (Bhat et al.,2019).

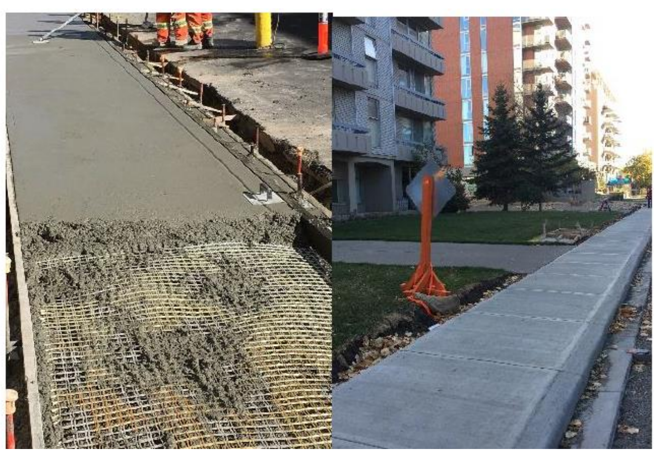

Figure 2.10 Using high-strength geogrid as concrete reinforcement for sidewalk in Calgary, Canada (Bhat et al.,2019).

2.5 Reinforced Embankment with Geotextile in Cold Temperature

Canada has the largest area of peatlands in the world. Peat is a highly compressible material with low shear strength, and high moisture content which causes excessive deformations and stability problems. Moreover, peat has a high organic content which affects the mechanical properties of peat over time and reducing its loading capacity. With cold temperatures, construction in peatland becomes more difficult while conventional design considerations are not enough to accommodate the problems related to frozen soil.

Guzman and Alfaro (2016) investigated the performance of two different construction methods of road embankment on seasonally frozen peat foundation to develop a more economical construction method. The project site was located 200 km southeast of Thompson in northern Manitoba, Canada. The study area was crossing over a large peat bag as shown in Figure 2.11 in April 2009.

Figure 2.11 Conditions along the road right-of-way in April 2009

(Guzman and Alfaro, 2016)

Figure 2.12a shows tested embankment with geotextile layer at its slopes (method A). To provide a separation layer between the fill materials and the underlying peat, the geotextile layer was placed on the surface of the peat before the fill materials was placed. The geotextile was wrapped around the side slopes from both sides to mobilize the tensile strength of the base geotextile in contact with peat as the peat foundation settles. The result from method A shows that approximately 30-40% of total height of the embankment has settled. Rowe et al., (1984) tested embankment and reported that immediate settlement was 50% of the total filling height. It can be concluded that Guzman and Alfaro (2016) method A reduced 10-20% of the immediate settlement, more than Maclean et al., (1984) method. Rowe et al., (1984) and Guzman and Alfaro (2016) concluded that geotextile can improve the embankment stability by reducing the lateral and vertical deformation of the embankment.

Method B is similar to method A with additional timber logs reinforcement as shown in Figure 2.12b. The embankment reinforced with both geotextile and timber log reduced the overall settlement and is more effective than reinforced with only geotextile.

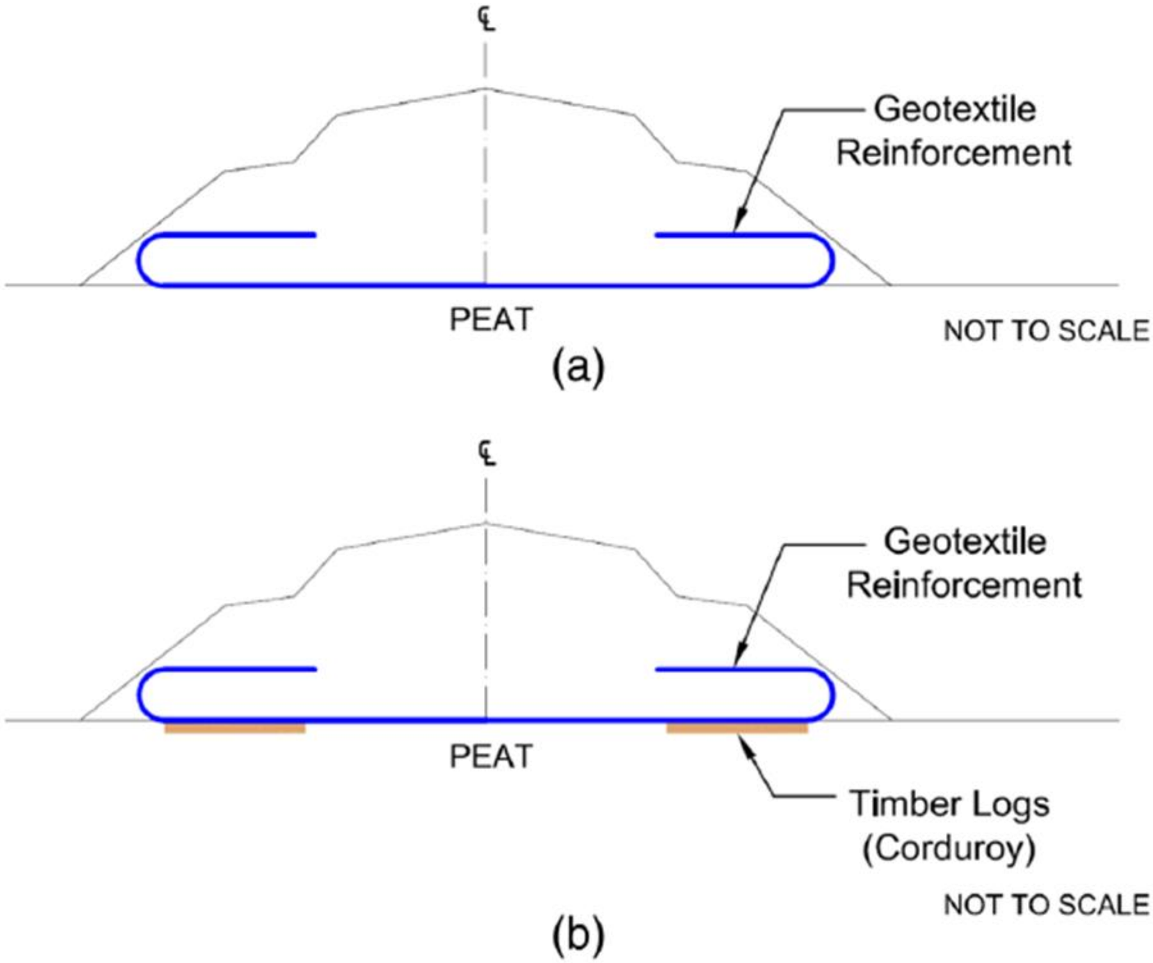

Figure 2.12 Embankment schematic diagram: (a) with geotextile (b) with geotextile and corduroy (Guzman and Alfaro, 2016)

2.6 Effect of Temperature on Fatigue of Polymers

Polymers are a relatively new materials in civil engineering which become an important supplement to conventional materials due to excellent chemical properties especially in highly corrosive environments. In the past two decades, a large number of studies have focused on studying the mechanical properties of polymers in extreme conditions.

Al-Kawi (2012) reported that tensile and fatigue stresses decreased by 46% with increasing of temperature from 40°C to 60°C after investigating the behavior of woven strand mats E-GF-reinforced polyester composites at temperatures 40°C, 50°C and 60°C.

Torabizadeh (2013) investigated the tensile behavior of unidirectional glass fiber (GF) reinforced epoxy matrix composites at room temperature (25°C), -20°C and -60°C. The tensile test results showed that the stress-strain curve decreases with increase in temperature.

Mortazavian and Fatmi (2015) Investigated the effects of temperature on cyclic deformation of fatigue behavior of two short fiber reinforced polymer composites (SFRPCs). One material is short glass fiber reinforced polybutylene terephthalate, containing 30 weight percent glass fibers (designated as PBT) and another material used is short glass fiber reinforced polyamide, with 35 weight percent glass fibers and 10 weight percent rubber (designated as PA6). Fatigue tests were conducted in samples of different thickness and different fiber orientation in longitudinal and transverse directions at -40°C, 23°C and 125°C. Results showed a significant effect of temperature in both directions. At the lowest testing temperature, the fatigue stress significantly increased. Figure 2.13 shows the effect of temperature where the horizontal axis represents the number of cycles to failure and the vertical axis represents fatigue stress for both materials in longitudinal and transverse directions. The effect of temperature in both materials was similar in both directions. Fatigue strength at 125°C significantly decreased compared to the 23°C.

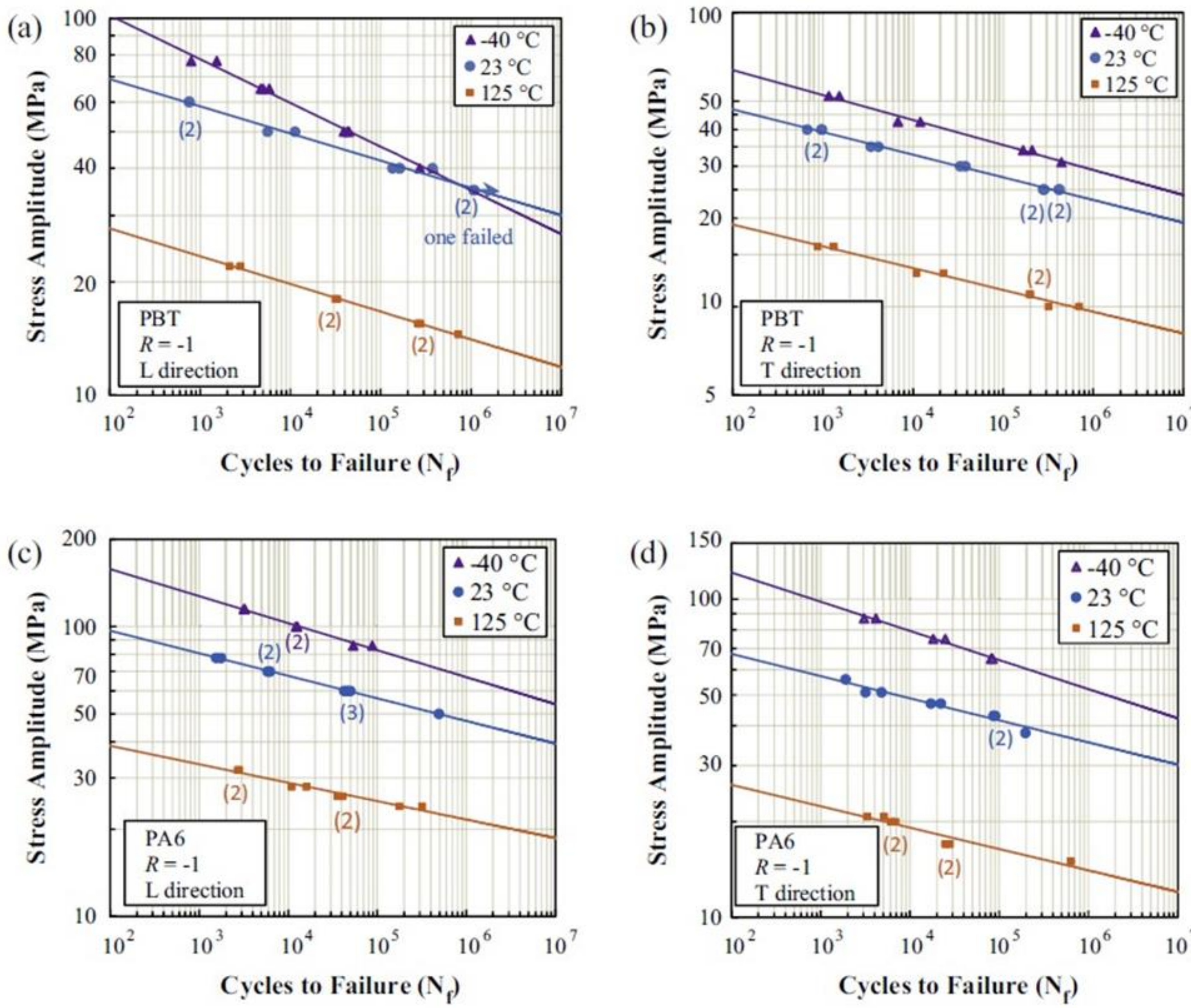

Figure 2.13 Effect of temperature for PBT in the (a) longitudinal and (b) transverse directions and for PA6 in the (C) longitudinal and (d) transverse directions

(Mortazavian and Fatmi, 2015)

Zhao and Wang (2018) investigated experimentally the tensile fatigue properties of glass fiber reinforced polymers (GFRP) used in civil engineering applications under high temperature. They tested a total of 105 bars in six different temperatures, namely, 100°C, 150°C, 200°C, 250°C, 300°C and 350°C, for a period of 0, 1 or 2 hours. The GFRP bars were tested under different cyclic load duration and temperature exposure. The results show that tensile strength decreases with the increase in holding time and temperature. Figure 2.14 shows the tensile strength in MPa and temperature from 0°C to 400°C in vertical axis and horizontal axis, respectively. For different holding periods, the tensile strength decreased with increase in temperature.

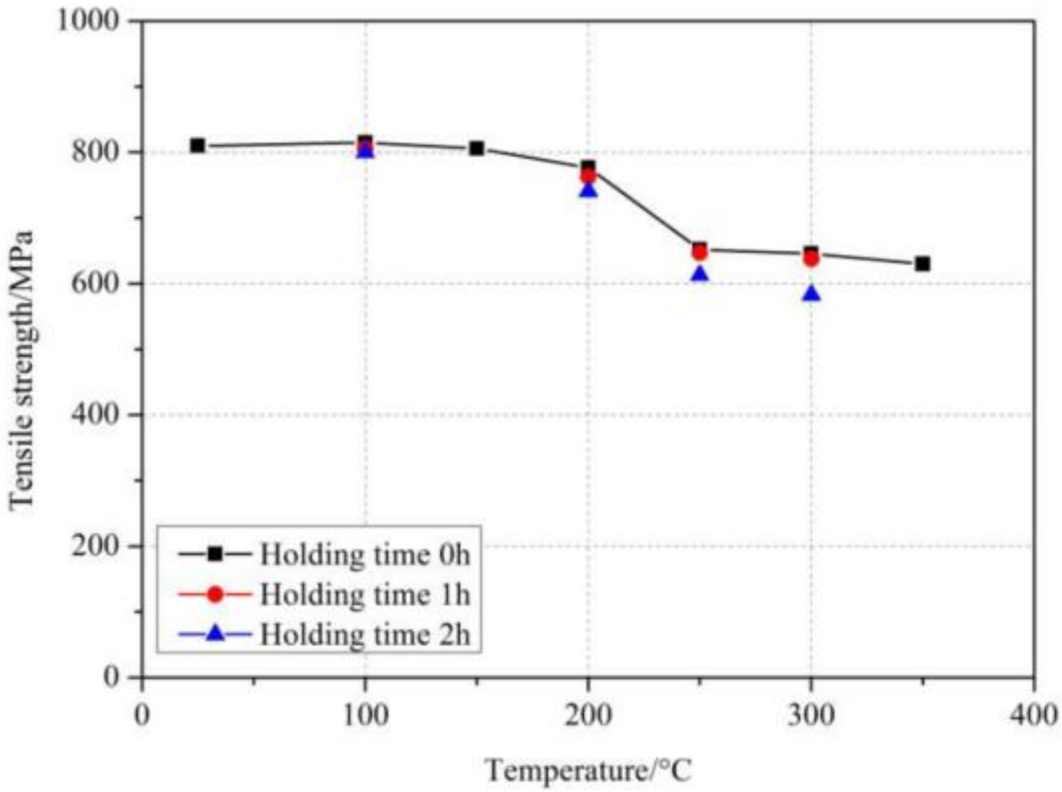

Figure 2.14 Tensile strength of GFRP with different holding time and elevated temperature (Zhao and Wang 2018)

2.7 Conclusions from the Literature Review

Based on the literature review, most of the conducted testes in the literature did not cover a temperature range that allows to examine the effect of compounding the negative and positive temperature. Moreover, the past studies are limited to polymeric geogrid. There is a need to expand these studies to cover the effect of thermal cycles on fiberglass geogrids.

2.8 Motivation of this Research

Fiberglass grid is a newly manufactured high-strength geogrid with material characteristics that seems to have the potential to serve for expanded applications under extreme environmental conditions. Thus, the goal of this study is to verify the fiberglass mechanical behavior under different temperature. Therefore, a series of experiments has been conducted to record the ultimate strength and strain. The result will be compared with conventional polymeric geogrid that presented in literature.

Chapter 3
Experimental program

3.1 Introduction

This chapter is divided into two sections. The first section presents the test setup and procedure used to investigate the effect of thermal cycles on the tensile response of high strength fiberglass geogrid (ConForce TE-SCR150). While the second section discusses the results of conventional polymeric biaxial geogrid (TE-BX40PP) subjected to the same thermal cycles. A total of seventy-two samples were tested in this experimental program with thirty-six samples for each the two examined geogrid materials.

The main variable of the test program is the number of cooling/heating cycles before the sample is tested. The test program consisted of six sets tests for each material including a control sample tested in room temperature (zero thermal cycles). Table 3.1 summarizes all conducted tests for fiberglass geogrid. The test parameters are explained and discussed in this chapter. The specimens were prepared and tested following ASTM D 6637 and using a standard MTS tensile machine located in the materials laboratory at McGill University.

Table 3.1. Conducted tests (Fiberglass geogrid)

	Number of samples	**Test type**
Test 1	6	0 cycles
Test 2	6	4 cycles
Test 3	6	8 cycles
Test 4	6	12 cycles
Test 5	6	16 cycles
Test 6	6	20 cycles
Total	36	

3.2 Investigation the Effect of Thermal Cycles on Fiberglass Geogrid

3.2.1 Thermal Capacity

Before commencing on the tensile test program, a series of tests has been conducted to evaluate the rate of temperature change of frozen geogrid with time. Samples were tested in a controlled temperature of -28°C for 48 hours. Thermocouples were connected to the freezer and subjected to ambient condition. This procedure was repeated for 3 different samples to find a repeatable Temperature-time (*T*-*t*) curve for these samples. Figure 3.1 shows the temperature time relation for fiberglass geogrid, where the horizontal and vertical axis represent the time in minutes and temperature ranges, respectively.

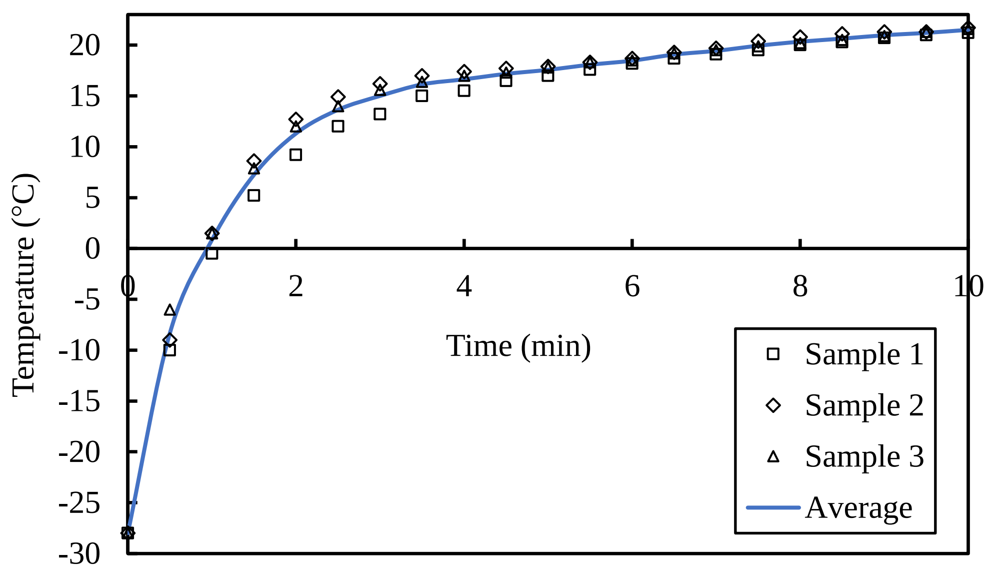

Figure 3.1. Temperature-time relationship for the fiberglass geogrid

The results obtained for all the three tested geogrid samples showed a constant rate of temperature change with time. The temperature was found to increase from -28°C to 0°C within a minute, while it took nine more minutes for the samples to reach room temperature (22°C).

these experiments reveal that the temperature of the fiberglass geogrid samples stabilizes, and the samples become ready for further testing if left in room temperature for more than ten minutes.

3.2.2 Tensile Tests

3.2.2.1 Material and Sample Preparation

The material tested is fiberglass biaxial geogrid with a trade name TE-SCR150 ConForce Grid, manufactured in India and supplied by Titan Environmental Containment, Manitoba, Canada. The geogrid has a thickness of 2.5 mm and contains high modulus fiberglass with durable polymeric coating manufactured using precision weaving process.

To prepare the material for testing, specimens measuring 250 mm were cut from a large sheet of supplied geogrid material (50 cm × 50 cm). Figure 3.2 shows the fiberglass geogrid sheets and the specimens that have been prepared for testing.

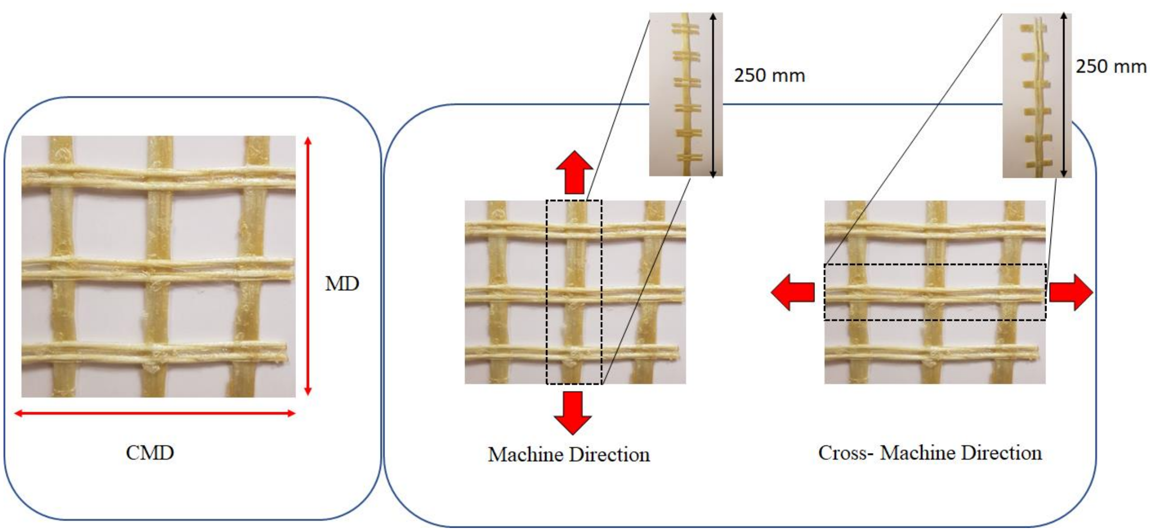

Figure 3.2. (a) Supplied geogrid sheet; (b) Tested specimen

3.2.2.2 Experimental Setup

A series of laboratory experiments was preformed to investigate the effect of freeze-thaw cycles on the tensile strength of fiberglass geogrid as well as the maximum strain at failure. The testing process starts with preparing the geogrid specimen with a total length of 250 mm. The prepared samples were frozen for 30 minutes to a temperature of -28°C and then left for 10 minutes at room temperature. This thermal cycle was repeated 4, 8, 12, 16, and 20 times to reach the number of cycles required.

All testing took place using a standard MTS machine located in the materials laboratory. Figure 3.3 shows the details of the MTS machine, which has a load cell capacity of 300 kN. To record the strains resulting from the sample loading, using a dedicated extensometer provides reliable data as compared to relying on the crosshead or the movement of the actuator as eliminates the possibility of measuring grip deflection, machine deflection or possible slippage. Therefore, a 50 mm gage length axial extensometer fixed to the specimen was used to measure the change in length during testing Figure 3.4.

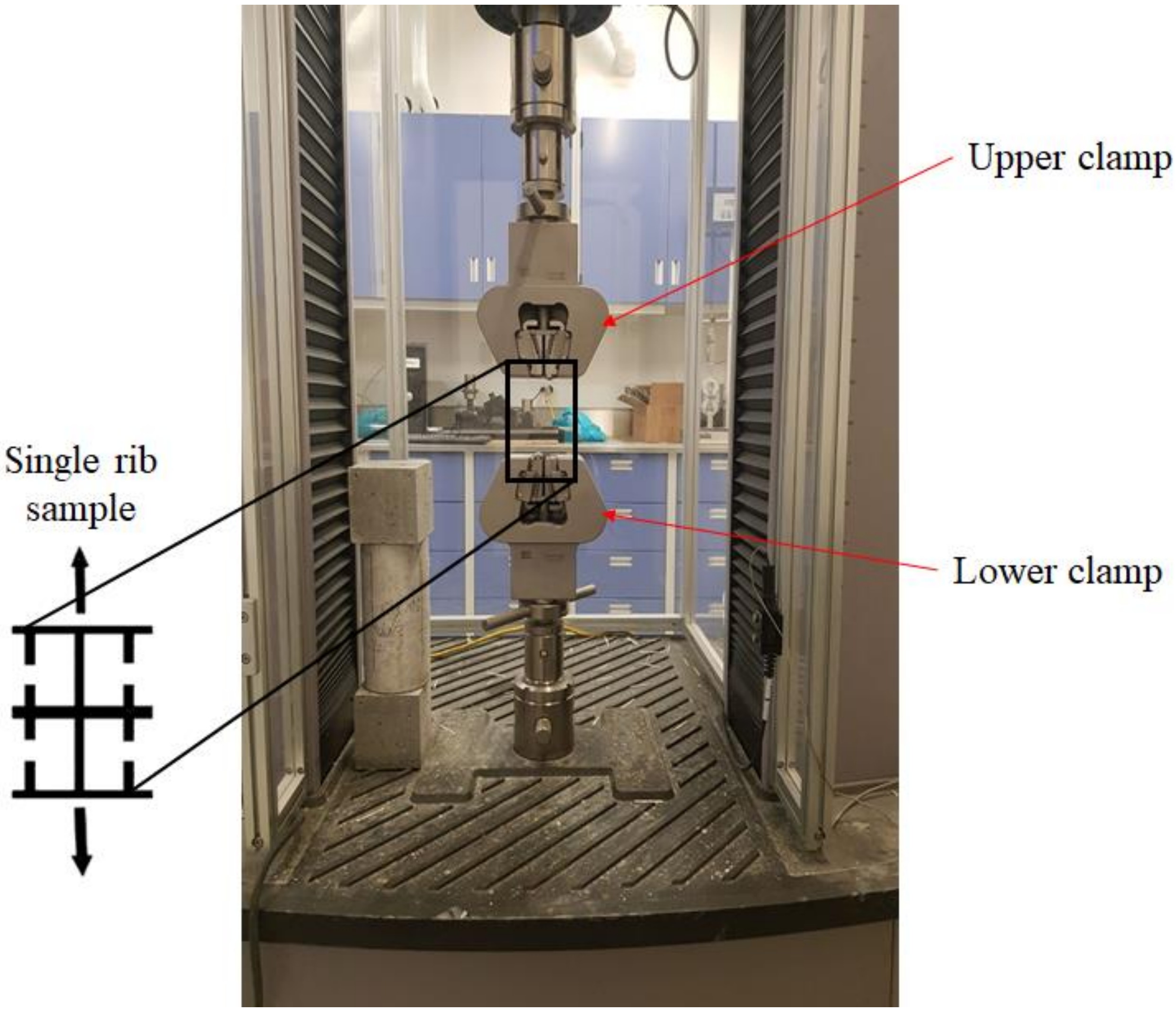

Figure 3.3. Details of the tensile test setup

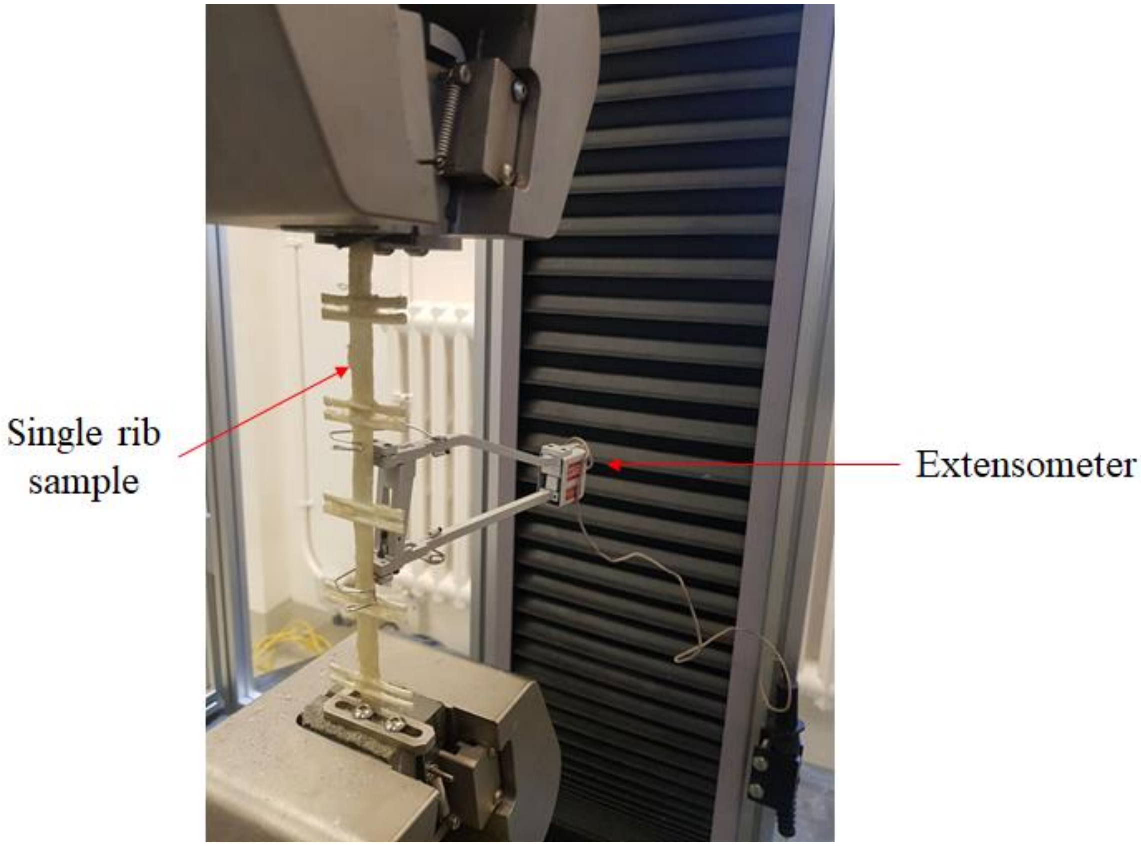

Figure 3.4. Extensometer

3.2.2.3 Testing Procedure

Single rib geogrid strength tests are performed following ASTM D 6637 test method. It involves applying an increasing load at a strain rate of 20 mm/ min to the tested sample up to failure. The objective of the test is to determine the maximum tensile stress that can be carried by the geogrid specimen before failure. This can be determined by measuring the maximum load divided by the specimen original cross section. Moreover, the sample elongation is also recorded for each load increment up to failure. The sample is tightly held by the lower and upper grips attached to the MTS machine. During the tensile test, the top grip is moved upward at a constant rate of 17 mm /min to pull and stretch the sample. The force and the corresponding elongation are continuously monitored to allow for a stress-strain relationship to be obtained. The machine stops as soon as the sample fails. The broken specimen is used to study the failure mode and overall behavior of the geogrid material.

3.2.2.4 Experimental Results

This section presents the experimental results of six thermal cycles. Different properties were measured, including the load capacity, the strains, and the failure modes.

3.2.2.4.1 Fiberglass Geogrid (Test 1) at Zero Cycles

Six geogrid samples were tested at room temperature without exposure to thermal cycles (control test). The results shown in this section will be used as a benchmark for the remaining tests. Table 3.2 summarizes the ultimate strength in kN/m and the strains for each sample along with the average strength for all tested samples. The average values for the ultimate strength and the corresponding strain were found to be 129.0 kN/m and 1.1%, respectively.

Table 3.2. Results under room temperature (Zero thermal cycles)

Sample number	**Ultimate strength (kN/m)**	**Strain at ultimate (%)**
1	127.4	1.1
2	127.0	1.0
3	137.1	1.2
4	124.2	1.1
5	141.5	1.1
6	122.2	1.0
Average	129.9	1.1

Figure 3.5 shows the tension-strain relationship for the six samples. The blue line represents the linear trend, which can be represented by $y = 116.65x$ [1], where $\boldsymbol{y}$ is the tension load in kN/m and $\boldsymbol{x}$ represents the strain in percentage. The trendline will be used to find the material's modulus of elasticity for the given cycle load.

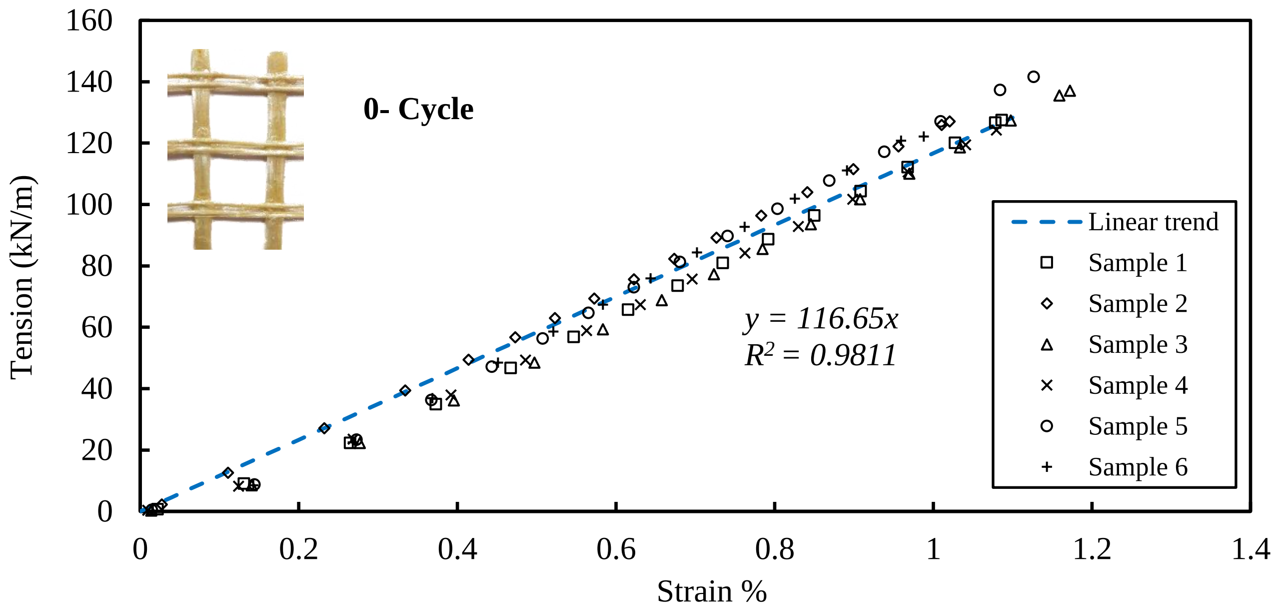

Figure 3.5. Tension strain relation for zero cycle

3.2.2.4.2 Fiberglass Geogrid (Test 2) after Four Thermal Cycles

Another six samples were tested after exposure to four complete freeze-thaw cycles for a total duration of 160 minutes. Table 3.3 shows the ultimate strength for each sample in kN/m, the average ultimate strength in kN/m and the corresponding strains, and average strain for each tested sample. The recorded average ultimate strength and the corresponding strain were 127.9 kN/m and 1.0%, respectively.

Table 3.3. Sample response following four thermal cycles

Sample number	Ultimate strength (kN/m)	Strain at ultimate (%)
1	121.45	0.8
2	133.43	1.0
3	133.07	1.0
4	126.02	0.9
5	127.55	1.0
6	125.91	1.3
Average	127.90	1.0

Figure 3.6 shows the tension strain curve for the six samples. The blue line represents the linear trend, which can be represented by $y = 120.95x$ [2], where $\boldsymbol{y}$ is the tension load in kN/m and $\boldsymbol{x}$ represents the strain in percentage. The trendline will be used to find the material's modulus of elasticity for the given cycle load.

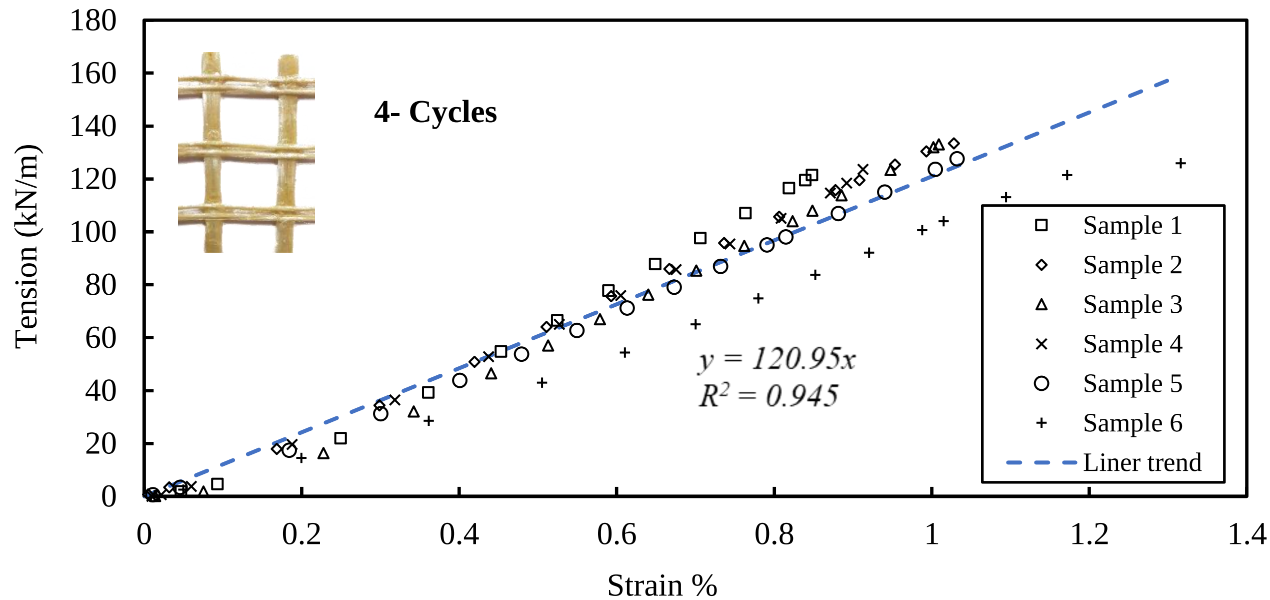

Figure 3.6. Tension-strain relationship after four cycles

3.2.2.4.3 Fiberglass Geogrid (Test 3) after Eight Cycles

After exposure to eight complete freeze-thaw cycles for a total duration of 320 minutes, six more samples were tested. Table 3.4 shows the ultimate strength for each sample in kN/m, the average ultimate strength in kN/m, strains at ultimate, and average strain values for all tested samples. The recorded average ultimate strength and strain at ultimate were found to be 127.8 kN/m and 1.0%, respectively.

Table 3.4. Sample response following eight thermal cycles

Sample number	**Ultimate strength (kN/m)**	**Strain at ultimate (%)**
1	137.46	1.1
2	125.82	0.9
3	132.60	1.0
4	124.98	1.0
5	128.02	1.0
6	118.03	0.9
Average	127.82	1.0

The stress-strain relationship for the six samples is demonstrated in Figure 3.7. The blue line represents the linear trend, which can be represented by $y = 129.65x$ [3], where $\boldsymbol{y}$ is the tension load in kN/m and $\boldsymbol{x}$ represents the strain in percentage. The slope of the trendline is used to define the material's modulus of elasticity for the applied load.

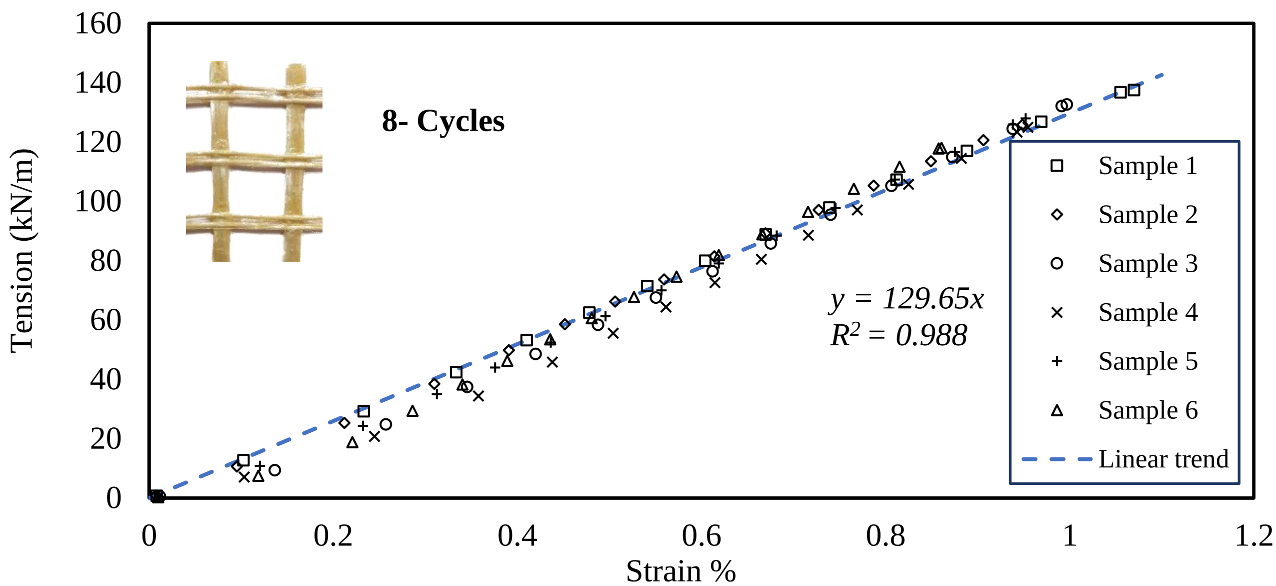

Figure 3.7. Tension-strain relationship after eight cycles

3.2.2.4.4 Fiberglass Geogrid (Test 4) after Eight Cycles

Again, six samples were tested after exposure to twelve complete freeze-thaw cycles for a total duration of 480 minutes. Table 3.5 shows the ultimate strength for each sample in kN/m, the average ultimate strength in kN/m, strain at ultimate strength, and average strain. The recorded average ultimate strength and the corresponding strain were found to be 128.1 kN/m and 1.1%, respectively.

Table 3.5. Sample response following twelve thermal cycles

Sample number	Ultimate Strength (kN/m)	Strain at Ultimate (%)
1	134.7	1.3
2	125.1	1.1
3	134.0	1.2
4	122.6	1.0
5	129.2	1.1
6	123.2	1.0
Average	128.1	1.1

Figure 3.8 shows the tension strain curve for six samples. The material's modulus of elasticity for this case is taken as define as the slope of the trendline (in blue). The linear trend can be represented by $y = 111.15x$ [4], where $\boldsymbol{y}$ is the tension load in kN/m and $\boldsymbol{x}$ represents the strain in percentage.

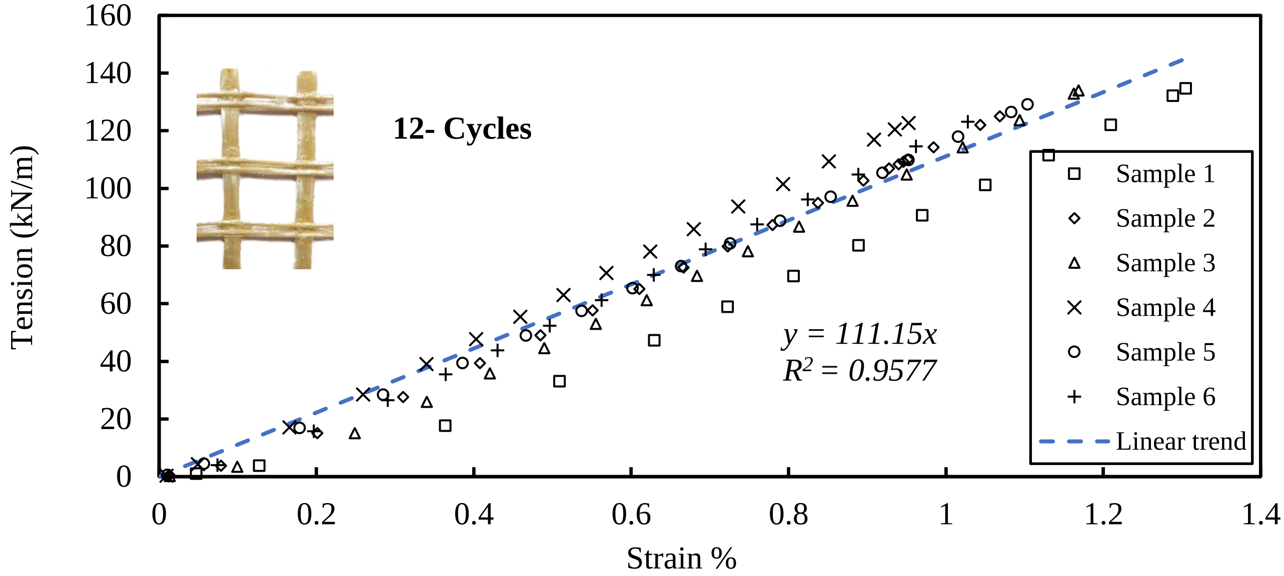

Figure 3.8. Tension-strain relationship after twelve cycles

3.2.2.4.5 Fiberglass Geogrid (Test 5) after Sixteen Cycles

After exposure to sixteen complete freeze-thaw cycles for a total duration of 640 minutes, six more samples were tested. Table 3.6 shows the ultimate strength for each sample in kN/m, the average ultimate strength in kN/m, strain at ultimate, and average strain. The recorded average ultimate strength and corresponding strain were 127.8 kN/m and 1.0%, respectively.

Table 3.6. Sample response after Sixteen thermal cycles

Sample number	Ultimate strength (kN/m)	Strain at ultimate (%)
1	140.45	1.1
2	129.44	1.1
3	125.84	1.0
4	134.13	1.1

5	112.59	0.9
6	135.3	1.0
Average	129.76	1.1

Figure 3.9 shows the tension strain curve for the six samples. The blue line represents the linear trend, which can be represented by $y = 115.83x$ [5], where y is the tension load in kN/m and x represents the strain in percentage. The trend line will be used to define the material's modulus of elasticity for the given cycle load.

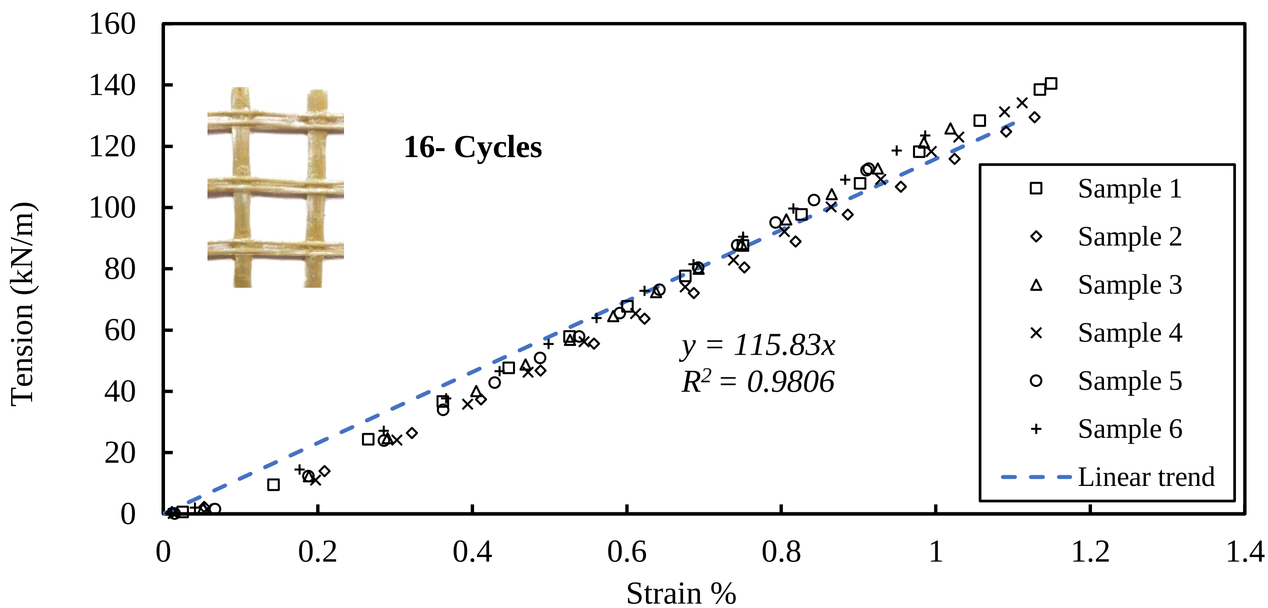

Figure 3.9. Tension-strain relationship after sixteen cycles

3.2.2.4.6 Fiberglass Geogrid (Test 6) after Twenty Cycles

After exposure to twenty complete cycles of freeze-thaw for a total duration of 800 minutes, another six samples were tested. Table 3.7 shows the ultimate strength for each sample in kN/m, the average ultimate strength in kN/m, strain at ultimate, and average strain. The recorded average ultimate strength and strain at ultimate were 129.8 kN/m and 1.1%, respectively.

Table 3.7. Sample response following twenty thermal cycles

Sample number	Ultimate strength (kN/m)	Strain at ultimate (%)
1	140.45	1.1
2	129.44	1.1
3	125.84	1.0
4	134.13	1.1
5	112.59	0.9
6	135.3	1.0
Average	129.76	1.1

Figure 3.10 shows the tension strain curve for the six samples. The blue line represents the linear trend, which can be represented by $y = 117.18x$ [6], where $\boldsymbol{y}$ is the tension load in kN/m and $\boldsymbol{x}$ represents the strain in percentage. The trend line will be used to define the material's modulus of elasticity for the given cycle load.

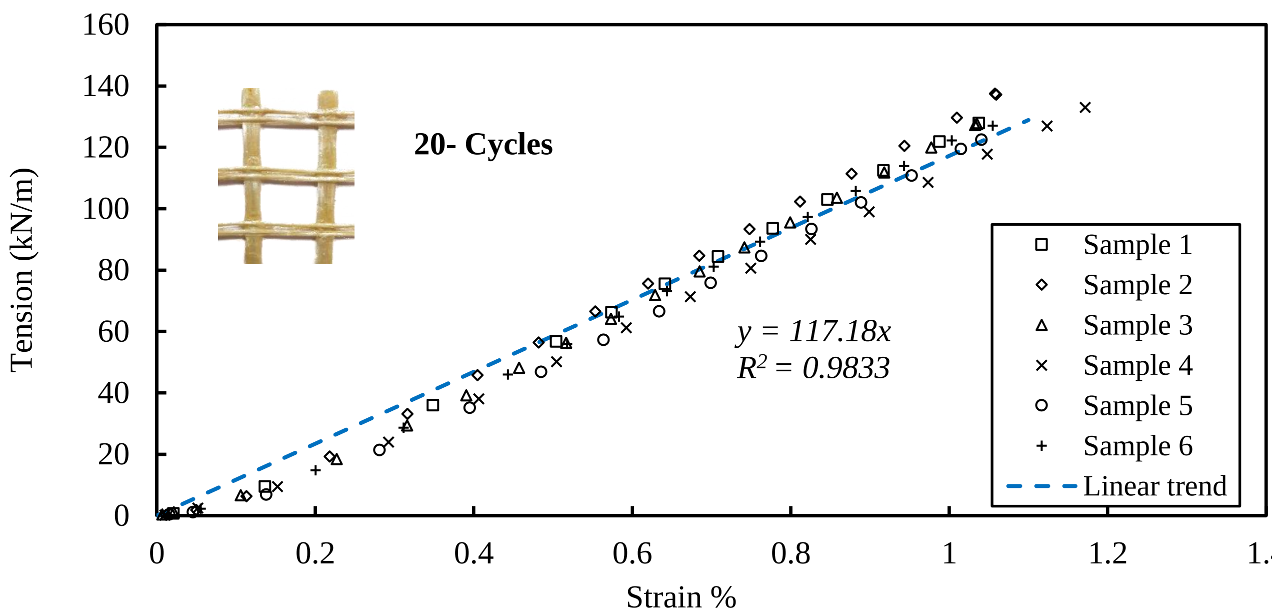

Figure 3.10. Tension-strain relationship after twenty cycles

3.3 Investigating the Effect of Thermal Cycles on Polymeric Geogrid

This Section presents the test details and procedure for 36 polymeric geogrid samples (**TE-BX40PP**) with different thermal cycles. Similar to fiberglass geogrid testing, the main variable of the test program was the number of cooling/heating cycles before the sample is tested. The test program consisted of six sets of six tests including a control sample tested in room temperature (zero thermal cycles). Table 3.8 summarizes all conducted tests for polymeric geogrid. The polymeric geogrid specimens were prepared and tested following ASTM D 6637 and using a standard MTS tensile machine located in the Materials laboratory at McGill University.

Table 3.8. Conducted tests (Polymeric geogrid)

	Number of samples	**Test type**
Test 1	6	0 cycles
Test 2	6	4 cycles
Test 3	6	8 cycles
Test 4	6	12 cycles
Test 5	6	16 cycles
Test 6	6	20 cycles
Total	36	

3.3.1 Thermal Capacity

To study the change of temperature with time, three samples of polymeric geogrid were frozen down to -28^{o} C for 48 hours. Then removed from the freezer to ambient condition. Thermocouples were connected to the sample to monitor its temperature, *T,* with time, *t*. Figure 3.11 shows the Temperature-time (T−t) curve for these samples and the average in green. The horizontal axis and vertical axis reflect, respectively, the time in minutes and the temperature in degree Celsius.

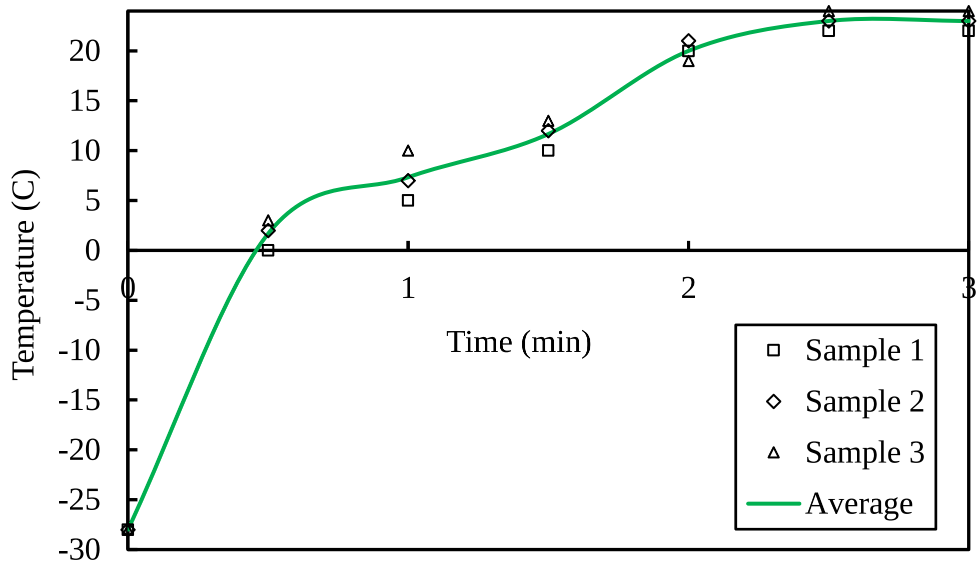

Figure 3.11. Polymeric geogrid Temperature-time curve

The results obtained for the three tested geogrid samples showed a constant rate of temperature change with time. The temperature was found to increase from -28ºC to 0 ºC within thirty seconds, while it took two and half more minutes to reach room temperature (22 º C). These experiments reveal that the temperature of the polymeric geogrid samples stabilizes, and the samples become ready for further testing if left in room temperature for more than three minutes.

3.3.2 Tensile Tests

3.3.2.1 Material and Sample Preparation

The material tested is baxial polymeric geogrid with a trade name (TE-BX40PP) Grid, manufactured in People's Republic of China and supplied by Titan Environmental Containment, Manitoba, Canada. The polymeric geogrid has a thickness of 2.5 mm and consists of processed polypropylene. Polymeric geogrid sheets are manufactured using a punching and drawing process whereby the polypropylene sheet is stretched in two directions, machine (longitudinal) (MD) and cross-machine (transverse) (CMD). The result is a monolithic and isotropic geogrid with thick and wide ribs, thick integral nodes, and uniform square apertures. The ribs have a high degree of molecular orientation continuing in part through the mass of the integral node. To prepare the material for testing, specimens measuring 300 mm were cut from a large roll of supplied material.

Figure 3.12 shows the polymeric biaxial geogrid sheets and the specimens prepared for testing.

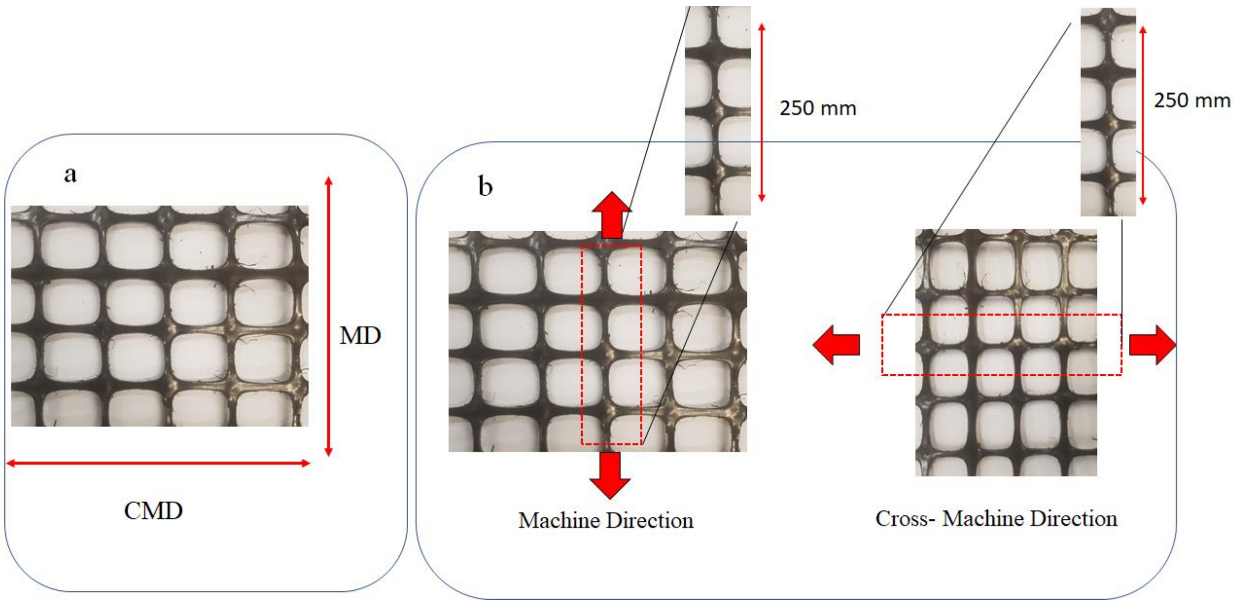

Figure 3.12.(a) Polymeric geogrid sheet (b) Tested specimen

3.3.2.2 Experimental Setup

A series of laboratory experiments was preformed to examine the effect of freeze-thaw cycles on the tensile strength of polymeric TE-BX40PP geogrid and the maximum strain at failure. Suchlike the testing process for fiberglass geogrid, polymeric geogrid specimens were cut into 250 mm as a required dimension. The prepared samples were frozen for 30 minutes to a temperature -28^{o}C and then left for 10 minutes at room temperature. This thermal cycle was repeated 4, 8, 12, 16, and 20 times to reach the number of cycles required.

All polymeric geogrid testing took place using the same MTS machine located in the materials laboratory which has been exhaustively introduced in the previous section.

A 50 mm gage length axial extensometer was used to record strain and measure the change in length during testing.

3.3.2.3 Testing Procedure

Following ASTM D 6637 test method introduced in the previous section, single polymeric rib samples were tested up to failure in order to determine the maximum tensile stress and ultimate strain using the MTS machine. The top grip is moved upward during the tensile test at a constant rate of 17 mm /min similar to the fiberglass geogrid rate. The force and the corresponding strain are continuously monitored to allow for a stress-strain relationship to be obtained. The MTS machine stops after specimen failure.

3.3.2.4 Experimental Results

This section presents the experimental results of six thermal cycles. Different properties were measured such as: the load capacity, strains and failure modes.

3.3.2.4.1 Polymeric Geogrid (Test 1) at Zero Cycles

Six polymeric geogrid samples were tested at room temperature without exposure to thermal cycles (control cycles test). The results shown in this section will be used as a benchmark for the remaining tests. Table 3.9 summarizes the ultimate strength in k/N and strains for each sample. The average values for the ultimate strength and the corresponding strain were found to be 52 kN/m and 7.6%, respectively.

Table 3.9. Results under room temperature (Zero thermal cycles)

Sample number	Ultimate strength (kN/m)	Strain at ultimate (%)
1	49.3	7.8

2	58.4	6.8
3	49.9	8.1
4	49.5	8.1
5	56.8	7.4
6	47.7	7.2
Average	51.9	7.6

Figure 3.13 shows the tension-strain relationship for the six samples. The green line represents second order polynomial trendline which will be used to find the material's modulus of elasticity for the given cycle load. The trendline can be represented by $y = -1.3048x^2 + 16.454x$ [7], where $\boldsymbol{y}$ is the tension load in kN/m and $\boldsymbol{x}$ represents the strain in percentage.

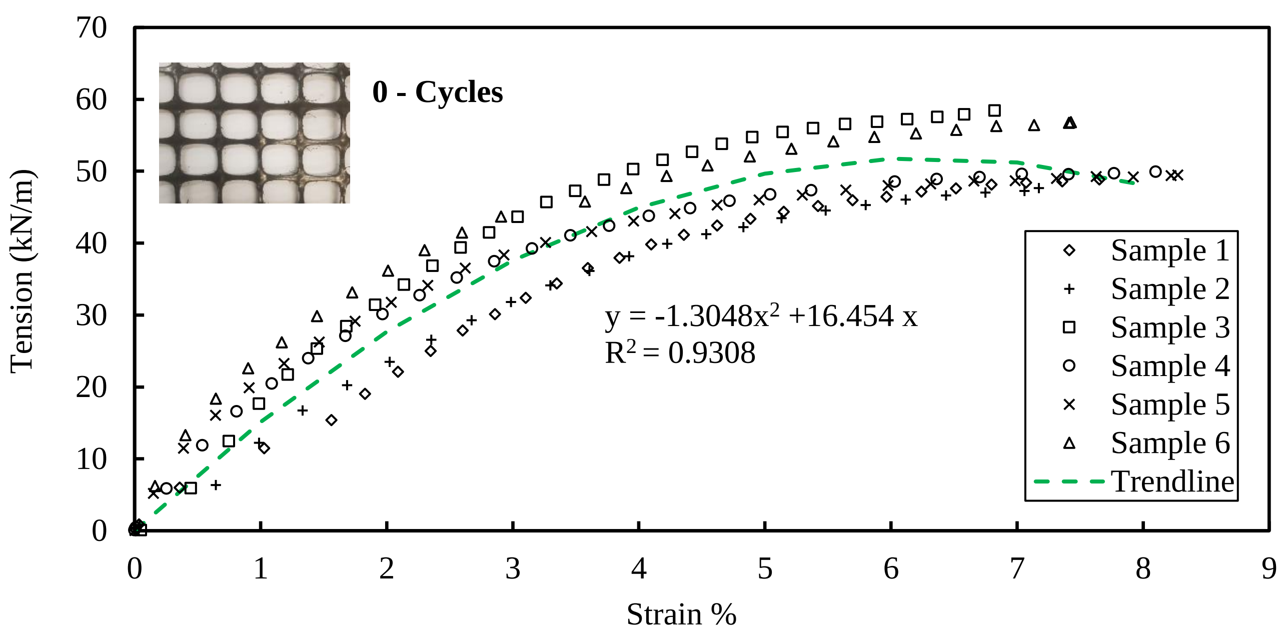

Figure 3.13. Tension strain curve for zero cycle

3.3.2.4.2 Polymeric Geogrid (Test 2) after Four Thermal Cycles

Another six polymeric geogrid samples were tested after exposure to four complete cycles of freeze-thaw for a total duration of 160 minutes. Table 3.10 shows the ultimate strength for each sample in kN/m, the average ultimate strength in kN/m, and the corresponding strains, and average strain of all tested samples. The recorded average ultimate strength and the corresponding strain were 49.1 kN/m and 7.9%, respectively.

Table 3.10. Sample response following four thermal cycles

Sample number	Ultimate strength (kN/m)	Strain at ultimate (%)
1	48.9	9.2
2	53.1	7.6
3	47.7	7.8
4	47.5	7.7
5	51.4	7.5
6	45.8	7.2
Average	49.1	7.9

Figure 3.14 shows the tension-strain relationship for the six samples. The green line represents second order polynomial trendline, which will be used to find the material's modulus of elasticity for the given cycle load. The trendline can be represented by $y = -1.4411x^2 + 16.969\,x$ [8], where $\boldsymbol{y}$ is the tension load in kN/m and $\boldsymbol{x}$ represents the strain in percentage.

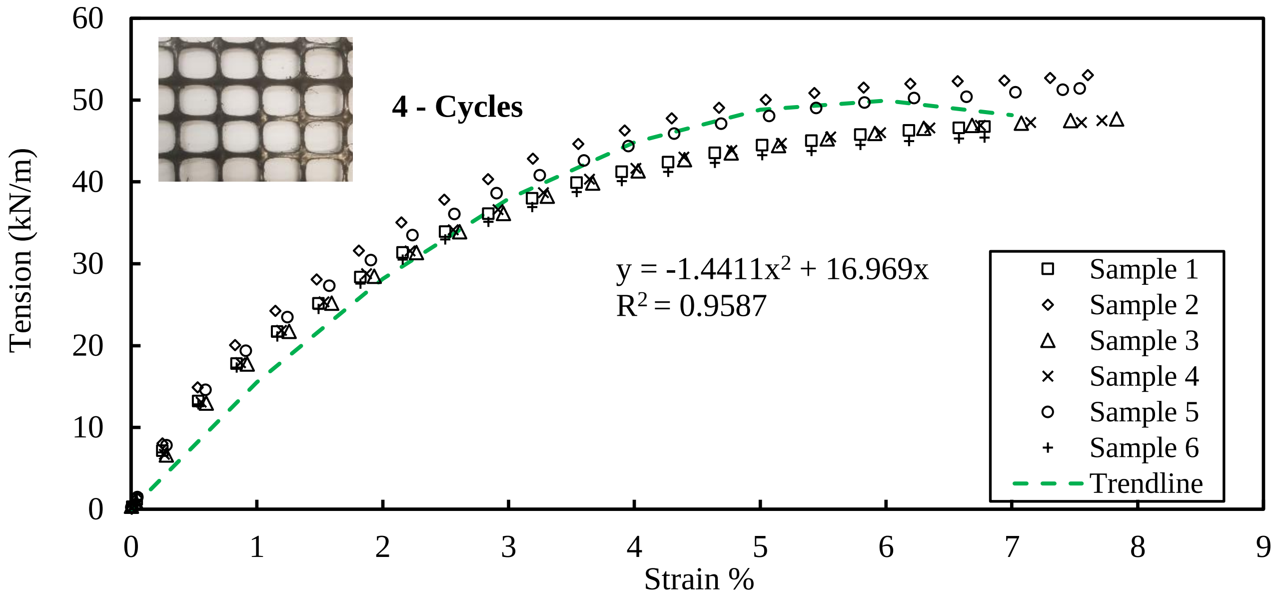

Figure 3.14. Tension-strain relationship after four cycles

3.3.2.4.3 Polymeric Geogrid (Test 3) after Eight Thermal Cycles

After exposure to eight complete freeze-thaw cycles for a total duration of 320 minutes, six more samples were tested. Table 3.11 shows the ultimate strength for each sample in kN/m, the average ultimate strength in kN/m, strains at ultimate, and average strain values for all tested samples. The recorded average ultimate strength and strain at ultimate were found to be 50 kN/m and 7.0%, respectively.

Table 3.11. Sample response following eight thermal cycles

Sample number	Ultimate strength (kN/m)	Strain at ultimate (%)
1	47.78	7.43
2	51.39	7.13
3	47.90	6.63
4	59.02	6.98
5	47.85	7.77
6	46.41	5.86
Average	50.06	6.97

Figure 3.15 shows the tension-strain relationship for the six samples. The green line represents second order polynomial trendline, which will be used to find the material's modulus of elasticity for the given cycle load. The trendline can be represented by $y = -1.6146x^2 + 18.162\,x$ [9], where $\boldsymbol{y}$ is the tension load in kN/m and $\boldsymbol{x}$ represents the strain in percentage.

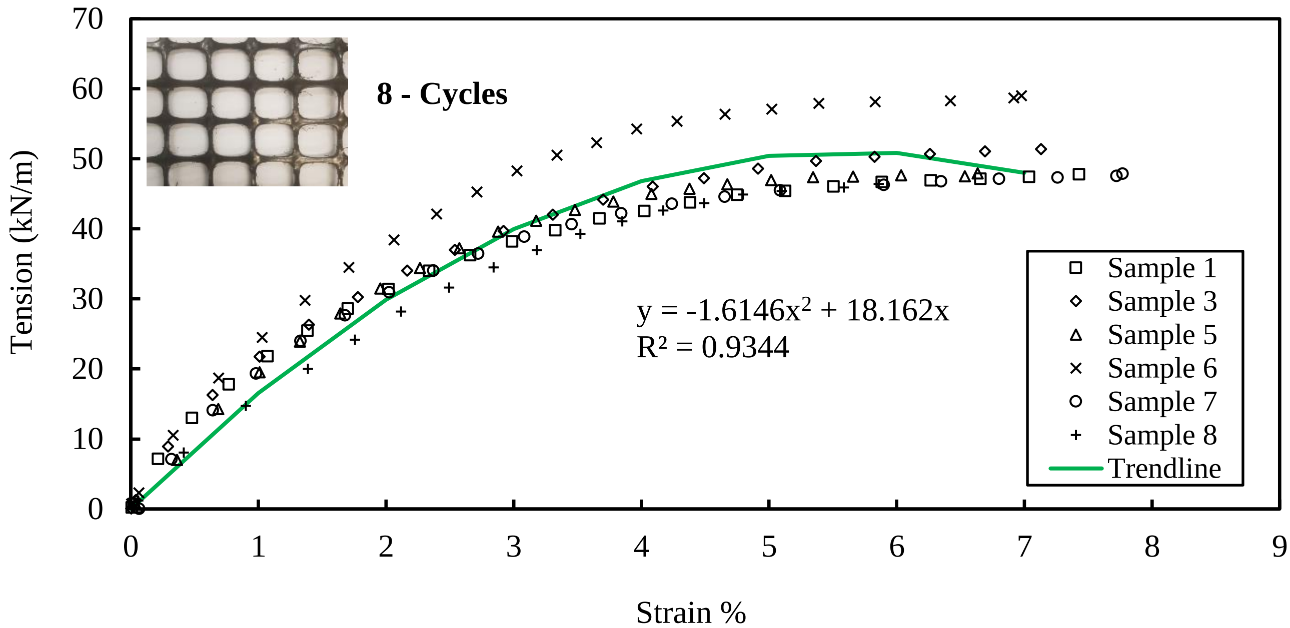

Figure 3.15. Tension-strain relationship after eight cycles

3.3.2.4.4 Polymeric Geogrid (Test 4) after Twelve Thermal Cycles

Again, six samples were tested after exposure to twelve complete freeze-thaw cycles for a total duration of 480 minutes. Table 3.12 shows the ultimate strength for each sample in kN/m, the average ultimate strength in kN/m, strain at ultimate strength, and average strain values for all tested samples. The recorded average ultimate strength and strain at ultimate were found to be 51.2 kN/m and 5.8%, respectively.

Table 3.12. Sample response following twelve thermal cycles

Sample number	Ultimate strength (kN/m)	Strain at ultimate (%)
1	49.9	5.4
2	45.3	5.0

3	47.0	5.6
4	48.2	4.5
5	49.1	7.6
6	52.3	6.7
Average	51.2	5.8

Figure 3.16 shows the tension strain curve for the six samples. The green line represents second order polynomial trendline, which will be used to find the material's modulus of elasticity for the given cycle load. The trendline can be represented by $y = -1.7469x^2 + 18.612x$ [10], where $\boldsymbol{y}$ is the tension load in kN/m and $\boldsymbol{x}$ represents the strain in percentage.

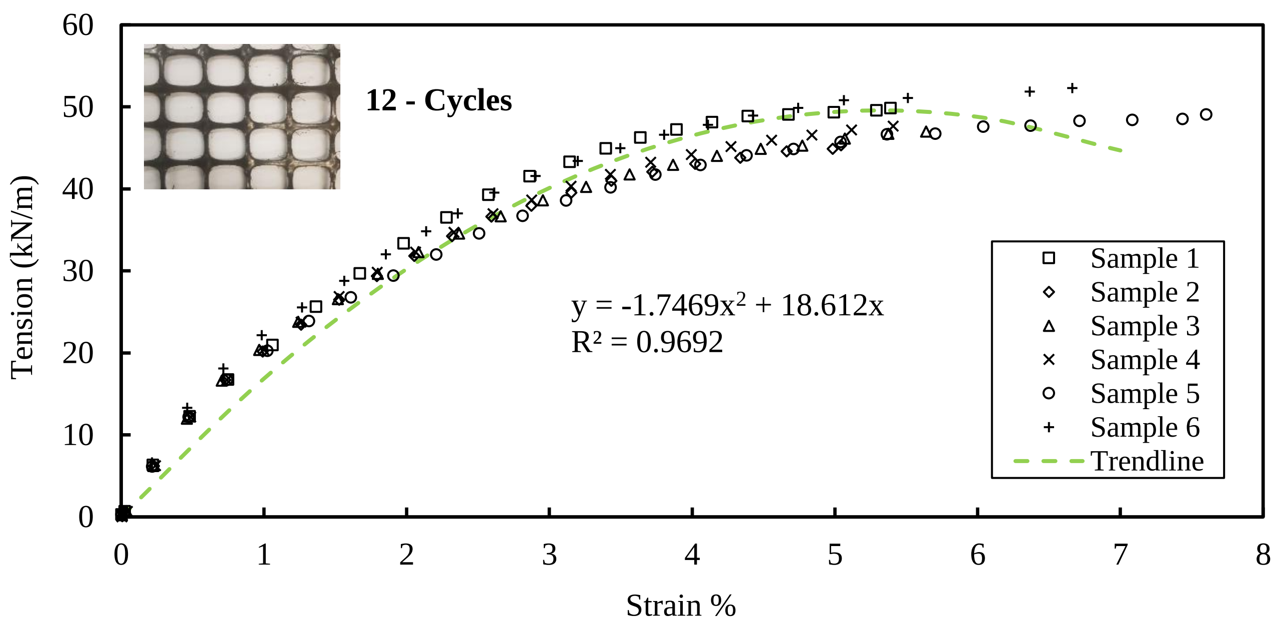

Figure 3.16. Tension-strain relationship for twelve cycles

3.3.2.4.5 Polymeric Geogrid (Test 5) after Sixteen Thermal Cycles

After exposure to sixteen complete freeze-thaw cycles for a total duration of 640 minutes, six more samples were tested. Table 3.13 shows the ultimate strength for each sample in kN/m, the average ultimate strength in kN/m, strain at ultimate strength, and average strain for all tested samples. The recorded average ultimate strength and the corresponding strain were 50.4 kN/m and 7.0%, respectively.

Table 3.13. Sample response following sixteen thermal cycles

Sample number	Ultimate strength (kN/m)	Strain at ultimate (%)
1	47.6	6.0
2	56.9	6.1
3	47.2	7.1
4	54.3	7.7
5	48.5	7.4
6	48.1	7.9
Average	50.4	7.0

Figure 3.17 shows the tension strain relationship for the six samples. The green line represents second order polynomial trendline, which will be used to find the material's modulus of elasticity for the given cycle load. The trendline can be represented by $y = -1.4508x^2 + 17.185x$ [11], where $\boldsymbol{y}$ is the tension load in kN/m and $\boldsymbol{x}$ represents the strain in percentage.

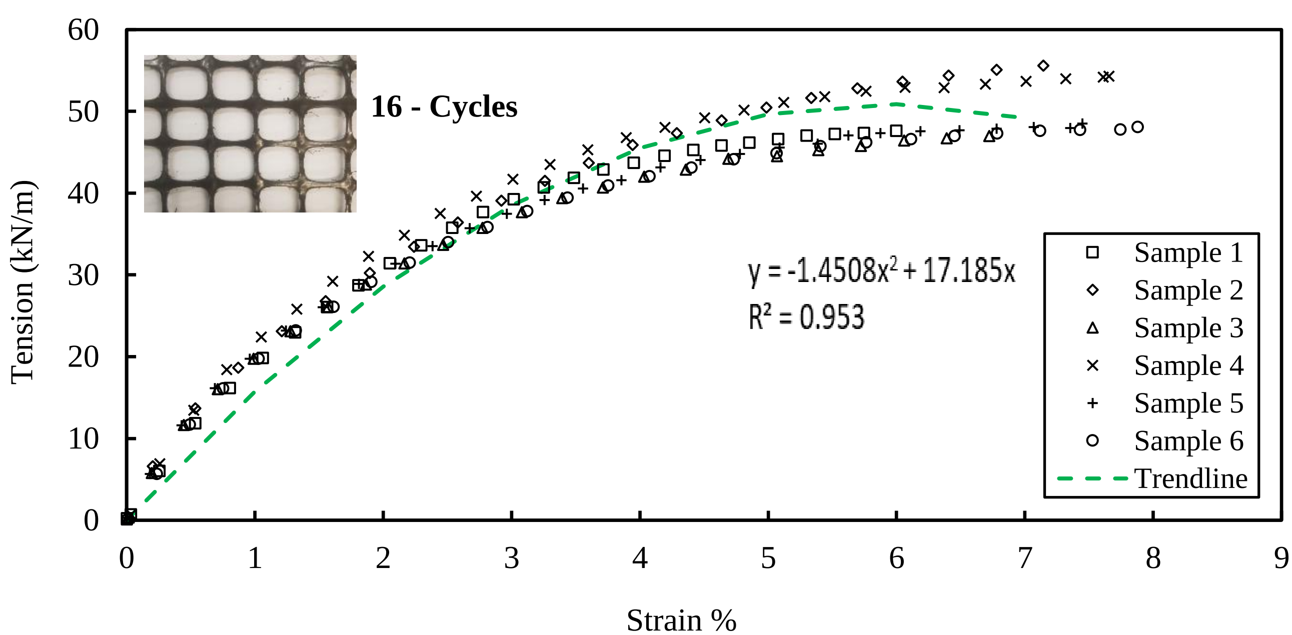

Figure 3.17. Tension-strain relationship after sixteen cycles

3.3.2.4.6 Polymeric Geogrid (Test 6) after Twenty Thermal Cycles

After exposure to twenty complete cycles of freeze-thaw for a total duration of 800 minutes, another six samples were tested. Table shows the ultimate strength for each sample in kN/m, the average ultimate strength in kN/m, strain at ultimate, and average strain. The recorded average ultimate strength and strain at ultimate were 50.2 kN/m and 7.6%, respectively.

Table 3.14. Sample response following twenty thermal cycles

Sample number	Ultimate strength (kN/m)	Strain at ultimate (%)
1	56.9	7.4
2	47.7	8.2
3	53.2	6.8
4	48.1	8.1
5	46.8	6.8
6	48.3	8.5
Average	50.2	7.6

Figure 3.18 shows the tension-strain relationship for the six samples. The green line represents second order polynomial trendline, which will be used to find the material's modulus of elasticity for the given cycle load. The trendline can be represented by $y = -1.4251x^2 + 17.049x$ [12], where $\boldsymbol{y}$ is the tension load in kN/m and $\boldsymbol{x}$ represents the strain in percentage.

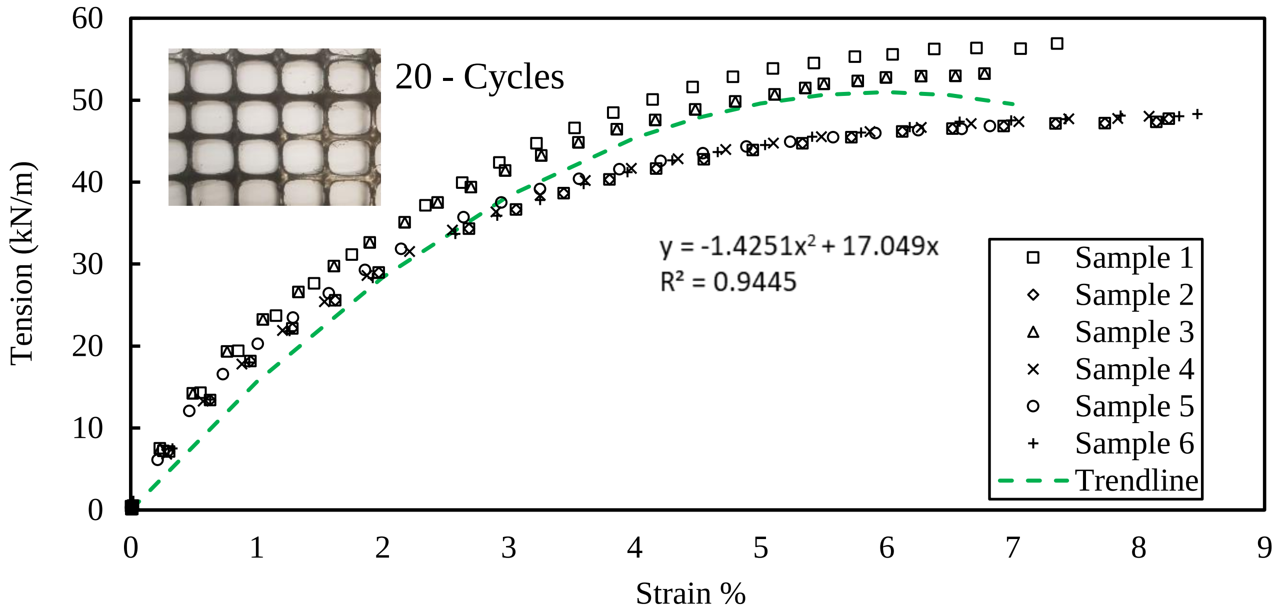

Figure 3.18. Tension-strain relationship after twenty cycles

Chapter 4

Discussion and Comparison

This chapter presents the discussion of the experimental results presented in chapter three for both the fiberglass and polymeric geogrids for all tested thermal cycles. The recorded measurements during all testing stages will be presented and discussed in this chapter. In addition, the chapter will also compare the responses of the two tested materials, including the ultimate strain, ultimate strength and modulus of elasticity.

4.1 Fiberglass Geogrid

Following the 36 fiberglass geogrid samples shown in chapter 3, table 4.1 summarizes the recorded properties for all the performed testing cycles from zero to twenty. The first two columns show the test number and the number of thermal cycles. The ultimate strength of a single rib is shown in the third column in (kN), while the fourth column shows the ultimate strength per meter (kN/m). The fifth and sixth columns show the strain at ultimate strength and the modulus of Elasticity in (MPa), respectively. The last row in the table shows the average of the entire column.

Table 4.1. All the fiberglass geogrid recorded properties

Test number	Number of cycles	Ultimate strength (kN)	Ultimate strength (kN/m)	Strain at ultimate strength (%)	Modulus of elasticity (MPa)
Test 1	0 Cycle	5.20	129.9	1.10	203.5
Test 2	4 Cycle	5.12	127.9	1.00	204.0
Test 3	8 Cycle	5.11	127.82	1.00	214.4
Test 4	12 Cycle	5.12	128.1	1.10	207.5
Test 5	16 Cycle	5.19	129.76	1.10	208.2

Test 6	20 Cycle	5.19	129.76	1.10	207.2
Average	-	5.15	128.87	1.07	208.5

4.1.1 Effect of Thermal Cycles on The Ultimate Strength

The control test (zero cycles) represents a condition where the tested material has not yet experienced any freeze-thaw cycles. The ultimate strength of the fiberglass geogrid at zero cycles is found to be about 130 kN/m. The ultimate strength per meter is found to decrease for the next two sets of tests (4 and 8 cycles) then slightly increase for the remaining sets of thermal cycles (12, 16 and 20 cycles). To understand the materials' trend, the ultimate strength of a single rib is evaluated as shown in the third column in table 4.1. The minimum and maximum values were 5.1 (8 cycles) and 5.20 (0 cycles), respectively. The maximum variation from the control tests is 1.7% at 8 cycles. The difference was found to decrease to about 1.5% at 4 and 12 cycles and continued to decrease until it reached 0.19% for 16 and 20 cycles. As the differences between the control tests and those involving thermal cycles is relatively small (less than %1.7), the material seems to be capable to maintain its ultimate strength even after multiple freeze-thaw cycles. Figure 4.1 shows the ultimate strength per single rib in each cycle.

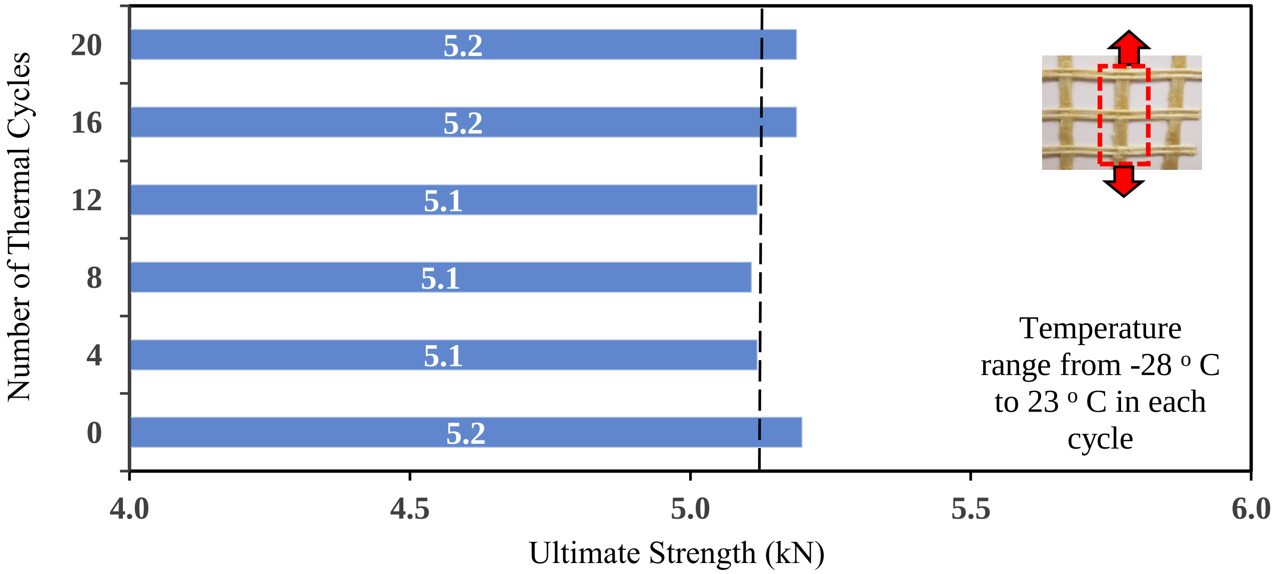

Figure 4.1 Ultimate strength for the tested single ribs in each tested cycle

4.1.2 Effect of Thermal Cycles on Strains

During testing, an extensometer is used to record the strains induced in the geogrid samples. The fifth column in table 4.1 shows the ultimate strain of all tested cycles. The strain values fall within 1% and 1.1% with an average of 1.07%, which indicates a stable strain with increasing the number of thermal cycles. In other words, the effect of thermal cycles on the material's strain is negligible. Figure 4.2 shows the ultimate strain per single rib in each thermal cycle

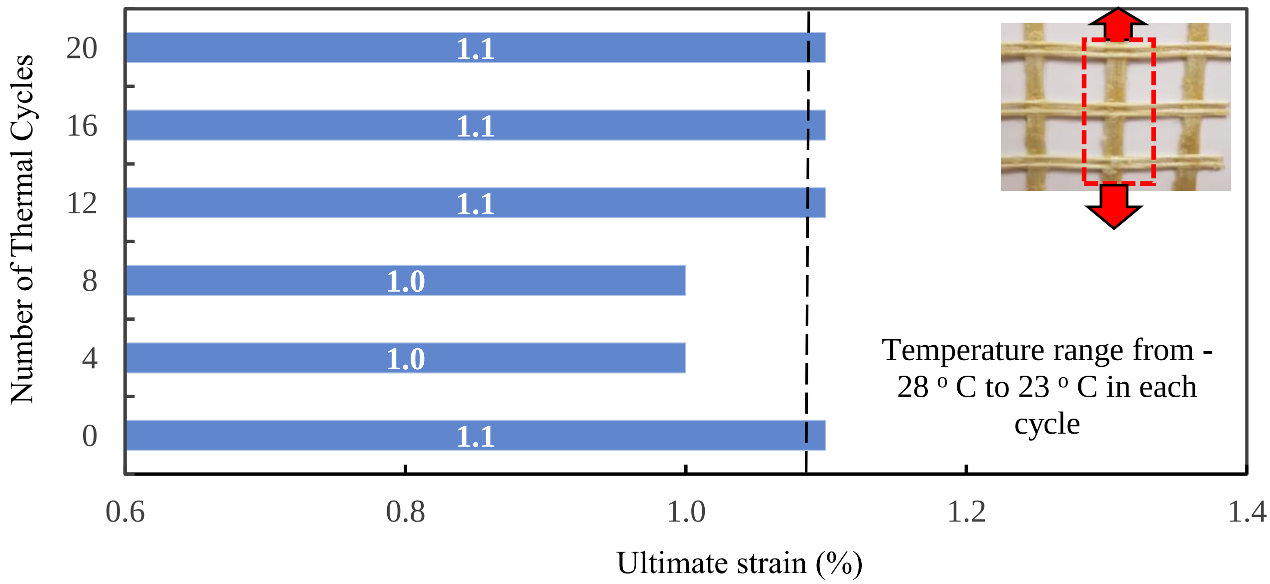

Figure 4.2 Fiberglass geogrid ultimate strain for each tested cycle

4.1.3 Effect of Thermal Cycles on the Modulus of Elasticity

The material's elastic modulus is taken as the slope of the linear portion of the stress-strain relationship in the elastic deformation range. All samples are found to reach failure in the elastic region. The last column in table 4.1 shows the calculated modulus of elasticity of each thermal cycle. The control test provided a modulus of elasticity is 203.5 MPa. The modulus value increased in all thermal cycles and reached its maximum value of 214.4 MPa at 8 cycles. Figure 4.3 shows the change in the modulus of elasticity for each test. The thermal cycles are shown to generally have a slightly positive effect on the material modulus. The slope of the line increased with the samples' exposure to thermal capacity cycles.

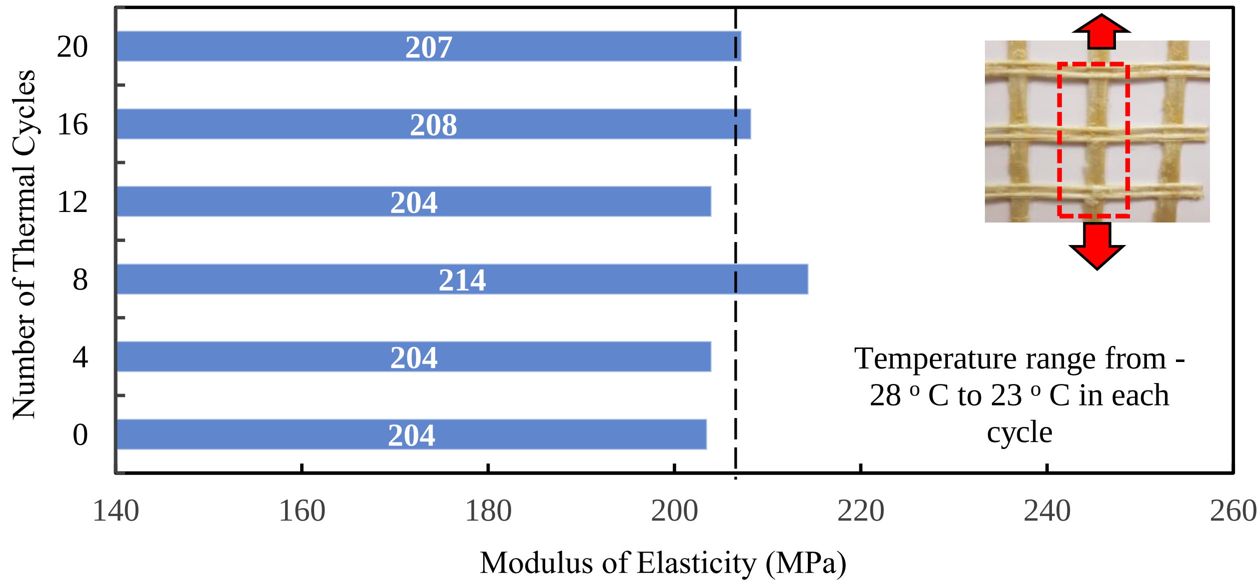

Figure 4.3 Value of the fiberglass geogrid modulus of elasticity for each cycle

4.2 Polymeric Geogrid

Based on the 36 tests performed on polymeric geogrid samples, table 4.2 presents the recorded properties for all tests involving thermal cycles from zero to twenty. The first two columns show the test number and cycles. The third, fourth and fifth columns show the ultimate strength per single rib in (kN), the ultimate strength per meter (kN/m), and the ultimate strains, respectively. The last column shows the material's modulus of elasticity in (MPa). The average values are shown at the last row of the table.

Table 4.2. All the polymeric geogrid recorded properties

Test number	Number of cycles	Ultimate strength (kN)	Ultimate strength (kN/m)	Strain at ultimate strength (%)	Modulus of elasticity (MPa)
Test 1	0 Cycles	1.5	51.9	7.6	23
Test 2	4 Cycles	1.4	49.1	7.9	21.1
Test 3	8 Cycles	1.4	50.06	6.97	25.1

Test 4	12 Cycles	1.5	51.2	5.8	27.7
Test 5	16 Cycles	1.4	50.4	7	24.3
Test 6	20 Cycles	1.4	50.2	7.6	22.4
Average		1.43	50.48	7.145	23.93

4.2.1 Effect of Thermal Cycles on the Ultimate Strength

Polymeric geogrid showed an ultimate strength of 52 kN/m before thermal cycles are applied (control tests). The maximum change in ultimate strength was found to be 5% at the 4 cycles test. The change decreased to 3% at 16 and 20 cycles and reached its minimum change of 1% at 12 cycles. The average ultimate strength is found to be about 50.5 kN/m. Neither did the material show a clear increasing nor decreasing trend with increasing the number of thermal cycles. However, at the maximum thermal cycles (20 cycles), the material strength slightly decreased by about 1%, which is considered insignificant. Figure 4.4 shows the ultimate strength in each cycle.

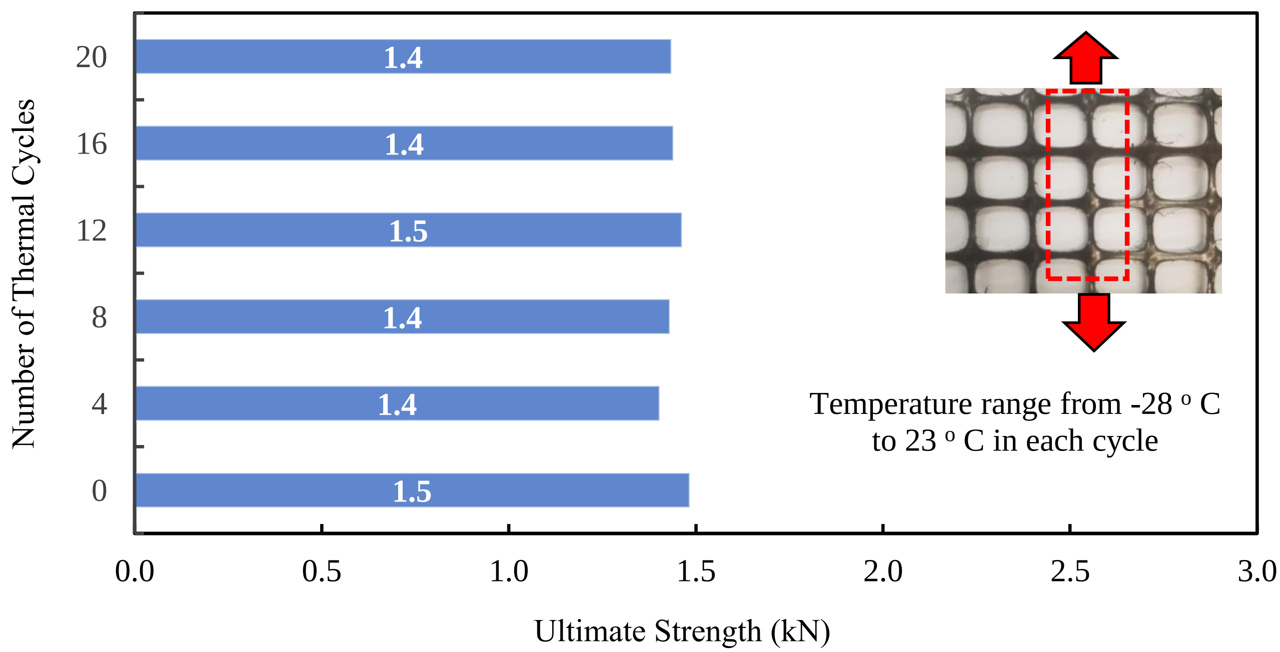

Figure 4.4 Ultimate strength for the tested single ribs

4.2.2 Effect of Thermal Cycles on Strains

As illustrated in Figure 4.5, the polymeric geogrid showed an ultimate strain equal to 7.6 % at zero cycles (control test) where the samples were never exposed to thermal cycles. The strain decreased by about 24% to reach 5.8% after 12 cycles while the maximum increase in strain was found to be 7.9 % after 4 cycles. The average strain for the conducted tests is found to be 7.1%. polymeric geogrid showed inconsistent relationship between the materials' strain and applied number of thermal cycles.

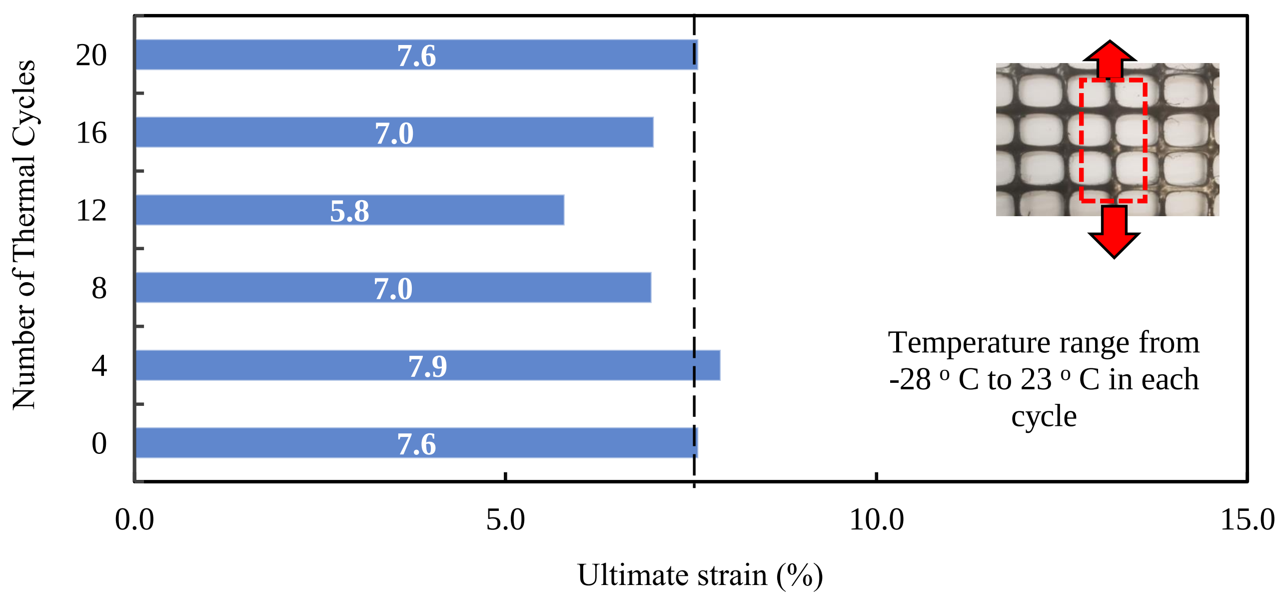

Figure 4.5 Polymeric geogrid ultimate strain for each tested cycle

4.2.3 Effect of Thermal Cycles on the Modulus of Elasticity

The minimum, maximum and average values of the modulus of elasticity of polymeric geogrid is found to be 21.1, 27.7 and 24 MPa, respectively. However, the control test provided a modulus of elasticity of 23 MPa. The maximum reduction in the elastic modulus is found to be 8% after 4 cycles. Figure 4.6 shows the modulus of elasticity for each test. The material showed a stable modulus of elasticity with the increase in the number of freeze- thaw cycles.

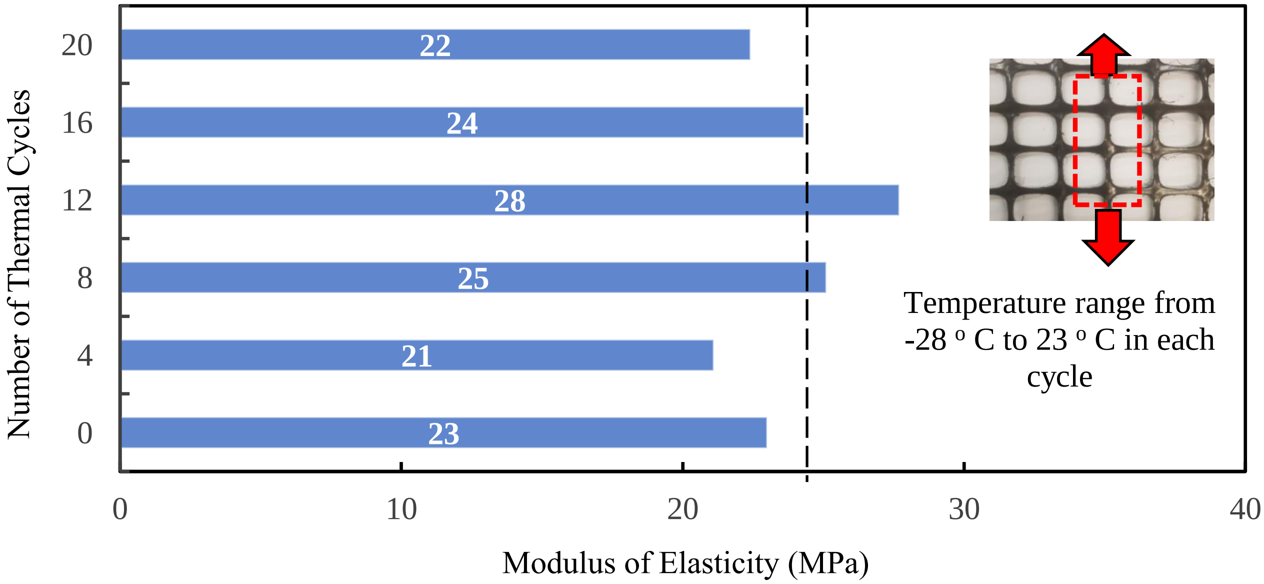

Figure 4.6 Polymeric geogrid modulus of elasticity for each cycle

4.3 Comparison between the tested Fiberglass and Polymeric Geogrids

In this section, a comparison between the fiberglass and polymeric geogrids is conducted. The purpose of the comparison is to evaluate the response of the newly manufactured fiberglass geogrid used in this study and compare it with the conventional polymeric geogrid. The comparison will be useful to recognize the difference in behavior of the two types of geogrids focusing on four elements: the ultimate strength per single rib, the ultimate strength per meter, the ultimate strain at failure and the modulus of elasticity.

4.3.1 Ultimate Strength for Single Rib

Both polymeric and fiberglass geogrids showed stable behavior with the increase in the number of thermal cycles. However, the fiberglass geogrid showed 5.3 kN average strength for a single rib, which is approximately four times that of the polymeric geogrid per single rib. Table 4.3 summarizes the ultimate strength values for each of the tests conducted for both materials as well as the average ultimate strength, while Figure 4.7 shows the ultimate strength-strain relationships for both materials. The blue line represents the average strength per rib for the fiberglass geogrid, while the orange line represents the results for the polymeric geogrid. The single rib of the fiberglass geogrid is found to be stiffer than that of the polymeric geogrid.

Table 4.3. Ultimate strength for fiberglass and polymeric geogrid for all thermal cycles

		Polymeric	**Fiberglass**
Test number	Number of cycles	Ultimate strength (kN)	Ultimate strength (kN)
Test 1	0 Cycles	1.5	5.2
Test 2	4 Cycles	1.4	5.1
Test 3	8 Cycles	1.4	5.1
Test 4	12 Cycles	1.5	5.1
Test 5	16 Cycles	1.4	5.2
Test 6	20 Cycles	1.4	5.2
Average	-	1.4	5.2

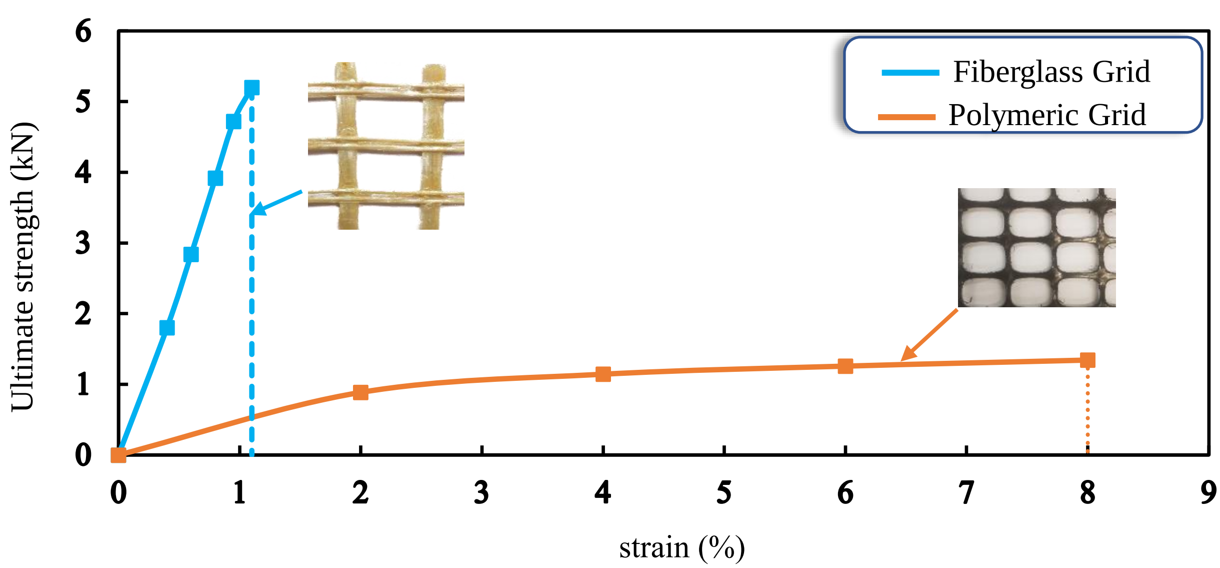

Figure 4.7 Fiberglass and polymeric geogrid strength-strain curve

4.3.2 The Ultimate Strength per Meter

It is noted that the geometry of the fiberglass geogrid is different compared to polymeric geogrid. In one-meter length, fiberglass geogrid contains 25 ribs, while the polymeric geogrid contains 35 ribs within the same unit length. This will increase the material's tension per unit length to reach an average of 129 kN/m and 50.5 kN/m for fiberglass and polymeric geogrid, respectively. Table 4.4 shows the complete ultimate tension per unit length for both materials in all tests as well as the average values.

Table 4.4. Ultimate strength per meter for all tests

		Polymeric	**Fiberglass**
Test number	**Number of cycles**	**Ultimate strength (kN/m)**	**Ultimate strength (kN/m)**
Test 1	0 Cycles	51.9	129.9
Test 2	4 Cycles	49.1	127.9
Test 3	8 Cycles	50.06	127.82
Test 4	12 Cycles	51.2	128.1
Test 4	16 Cycles	50.4	129.76
Test 4	20 Cycles	50.2	129.76
Average	-	50.48	128.87

In Figure 4.8, the ultimate strength is shown in blue and orange for both the fiberglass and polymeric geogrid, respectively. The ultimate strength for the fiberglass geogrid outperforms that of polymeric geogrid by 2.5 times for the same unit length.

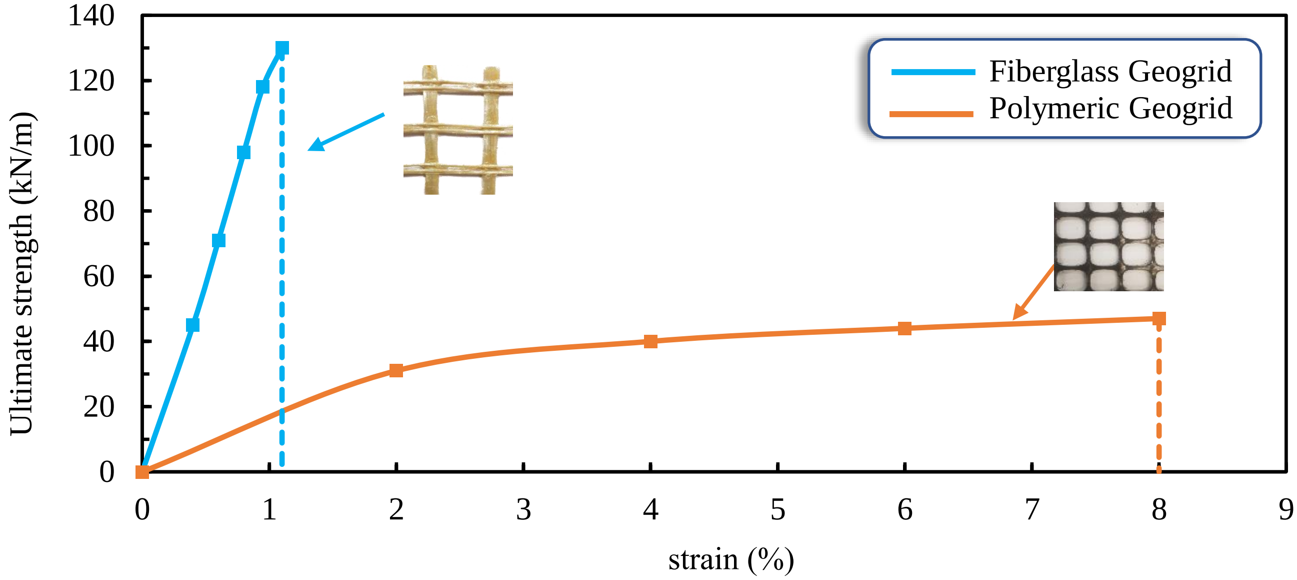

Figure 4.8 Fiberglass and polymeric strength-strain relation

4.3.3 Ultimate Strain at Failure

It is noted that the thermal cycles did not show significant effect on the ultimate strain of both tested materials. However, the ultimate strain is 1% and 8% for the fiberglass and polymeric geogrids, respectively, which means that the ultimate strain of the fiberglass geogrid is 7 to 8 times lower than that of the polymeric geogrid. Table 4.5 shows the strain values measured for both materials together with the average values.

Table 4.5. Ultimate strain for all tests

		Polymeric	**Fiberglass**
Test number	**Number of Cycles**	**Strain at Ultimate (%)**	**Strain at Ultimate (%)**
Test 1	0 Cycles	7.6	1.1
Test 2	4 Cycles	7.9	1.0
Test 3	8 Cycles	7.0	1.0
Test 4	12 Cycles	5.8	1.1
Test 5	16 Cycles	7.0	1.1

Test 6	20 Cycles	7.6	1.1
Average	-	7.145	1.07

4.3.4 Modulus of Elasticity

The modulus of elasticity represents a specific material's resistance to deformation. The fiberglass geogrid shows a brittle behavior as the tension strain curve is linear. However, the polymeric geogrid shows more ductility behavior and more capability to elongate. With the increase in the number of thermal cycles, both materials showed minor change in their modulus of elasticity. However, polymeric geogrid showed only 24 MPa, while the fiberglass geogrid showed an average modulus of 207 MPa, which is approximately 8.6 times the polymeric modulus. Table 4.6 shows the complete set of values for the modulus of elasticity in all tests conducted for both materials.

Table 4.6. Modulus of elasticity for both the fiberglass and polymeric geogrids

		Polymeric	**Fiberglass**
Test number	Number of Cycles	Modulus of Elasticity (MPa)	Modulus of Elasticity (MPa)
Test 1	0 Cycles	23	203.5
Test 2	4 Cycles	21.1	204
Test 3	8 Cycles	25.1	214.4
Test 4	12 Cycles	27.7	204
Test 5	16 Cycles	24.3	208.23
Test 6	20 Cycles	22.4	207.23
Average	-	23.93	206.9

Chapter 5
Conclusion and Recommendation

5.1 Conclusions

The effect of thermal cycles on the mechanical properties for the conventional polymeric geogrid as well as the newly manufactured high-strength fiberglass geogrid were investigated using experimental testing. The experimental program included testing of 72 samples from both materials exposed to different thermal cycles that range from 0 to 20 cycles. Based on the results and discussions, the following conclusions can be drawn:

- For the control tests (no thermal cycles), the fiberglass geogrid showed ultimate strength per single rib that is 3.5 times that of the polymeric geogrid.
- For all applied thermal cycles, the fiberglass geogrid showed ultimate strength that is 3.4 to 3.6 times that of the polymeric geogrid. Both materials showed a stable strength with the increase in the number of thermal cycles from 4 to 20.
- Fiberglass geogrid showed ultimate strength per meter length that is 2.6 times higher than that of the polymeric geogrid for the control test.
- For the control test (no thermal cycles), the fiberglass geogrid shows 7 times the polymeric geogrid ultimate strain.
- For all tests involving thermal cycles, the fiberglass geogrid showed a maximum ultimate strain at failure of 1.1%.
- Fiberglass and polymeric geogrids showed modulus of elasticity equivalent to 204 MPa and 23 MPa, respectively, in the control tests.

- Both materials showed slight changes in their modulus of elasticity with the increase in the number of thermal cycles. However, for all tests, the fiberglass geogrid showed modulus of elasticity that is 7.3- 9.7 times higher than that of the polymeric geogrid.

5.2 Recommendations

Based on this study, the following recommendations for further research can be made:

- Expand the experimental investigation to cover more mechanical properties, e.g. the hardness of the geogrid.
- Conducting tensile tests inside a temperature-controlled chamber and study the effect of temperature on the mechanical properties of the geogrids.
- Change the number of thermal cycles up to 100 thermal cycles to capture any effect of thermal cycles on the tensile behavior of the geogrids.
- Expand the experimental investigation to explore the use of fiberglass geogrid as reinforcement material for ground supported structural elements in cold climate.

References

Allen, T., Bell, J.R. and Vinson, T.S. (1983), "Properties of Geotextiles in Cold Regions Applications", Transportation Research Record, Report No. 83-6, Transportation Research Institute, Oregon State University, Corvallis, OR.

Bhat, S., & Thomas, J. (2015). Use of Polymer Geogrid Composite to support rail track over weak saturated clay subgrade–a case study.

Bhat, S., Thomas, J., & Lakkavalli, V. (2015). Design and construction of a geosynthetic reinforced pavement on weak subgrade.

Bhat, S., Thomas, J., & Skrobutan, R. (2013). Use of polymer Geogrid reinforcement in the foundations of ground supported tanks for control of differential settlement.

Bhat, S., Thomas, Jimmy;, and Venkat Lakkavalli,. (2019). Pilot Case Study of Geogrid Reinforcement in Concrete.

Calhoun, C. C. (1972). Investigation of plastic filter cloths. Oklahoma State University, De Guzman, Earl Marvin B

De Guzman, E.M.B., Alfaro, M., 2016. Performance of road embankments on seasonally frozen peat foundations with and without corduroy bases. J. Perform. Constr. Facil. 30 (6), 1–9.

Hsieh C, Tseng Y. Tensile creep behavior of a PVC coated polyester geogrid at different temperatures. J GeoEng 2008;3(3):113–9.

Hussain J. Al-alkawi, D. S. A.-F. a. A.-J. H. A. (2012). Fatigue behavior of woven glass fiber reinforced polyester under variable temperature. Elixir International Journal, 53.

Koda, E., Miszkowska, A., & Kiersnowska, A. (2018). Assessment of the temperature influence on the tensile strength and elongation of woven geotextiles used in landfill.

Kongkitkul, W., Tabsombut, W., Jaturapitakkul, C., & Tatsuoka, F. (2012). Effects of temperature on the rupture strength and elastic stiffness of geogrids. Geosynthetics international, 19(2), 106-123.

Li, G., Zhao, J., & Wang, Z. (2018). Fatigue behavior of glass fiber-reinforced polymer bars after elevated temperatures exposure. Materials, 11(6), 1028.

Mortazavian, S., & Fatemi, A. (2015). Fatigue behavior and modeling of short fiber reinforced polymer composites including anisotropy and temperature effects. International Journal of Fatigue, 77, 12-27.

SGI testing services. (2020). Tensile properties under 20°C and under - 20°C conditions, Titan Geogrid (Report No. SGI19022.report.2020.03)

Palmeira, E. M., Tatsuoka, F., Bathurst, R. J., Stevenson, P. E., & Zornberg, J. G. (2008). Advances in geosynthetics materials and applications for soil reinforcement and environmental protection works. Electronic Journal of Geotechnical Engineering, 13.

Rowe, R., MacLean, M., & Soderman, K. (1984). Analysis of a geotextile-reinforced embankment constructed on peat. Canadian Geotechnical Journal, 21(3), 563-576.

Torabizadeh, M. A. (2013). Tensile, compressive and shear properties of unidirectional glass/epoxy composites subjected to mechanical loading and low temperature services.